Bulletin of the Geological Survey of Japan, vol.61 (11/12), p.383-415, 2010

Article

# Petrochemistry of I-type magnetite-series granitoids of the northern Chile, Highland Valley, southern B. C., Canada, Erdenet mine, Mongolia, Dexing mine, China, Medet mine, Bulgaria, and Ani mine, Japan

Shunso Ishihara[1, *] and Bruce W. Chappell[2]

Shunso Ishihara and Bruce W. Chappell (2010) Petrochemistry of I-type magnetite-series granitoids of the northern Chile, Highland Valley, southern B. C., Canada, Erdenet mine, Mongolia, Dexing mine, China, Medet mine, Bulgaria, and Ani mine, Japan. *Bull. Geol. Surv. Japan*, vol.61 (11/12), p.383-415, 15 figs, 1 table, 3 appendixes.

**Abstract:** Granitoids from porphyry copper mineralized regions from selected areas in the world were reexamined by the polarized X-ray method. The studied samples in Chile include regional collection of three transects, North, Central and South, including Chuquicamata, El Salvador, Rio Blanco-Los Blances and El Teniente mines. The east-west variation in younging the age toward east is best shown in the North and Central transects. Components that tend to increase toward the inner direction are $Al_2O_3$, $Na_2O$, $P_2O_5$ and Sr, while those of decreasing are Y, total Fe and V. The innermost is a zone of porphyry copper deposits. Therefore, high Sr/Y granitoids prevail in the innermost and youngest zone.

Other porphyry copper regions studied include granitoids from Highland Valley copper area, southern B. C., Canada, Erdenet mine of Mongolia, Dexing mine of China, Medet mine of Bulgaria, and Ani mine stock of Japan. The studied samples all belong to I-type magnetite-series, according to their magnetic susceptibility and bulk $Fe_2O_3$/FeO ratio, and major chemistry. ASI is less than 1.1 (i.e., I-type), except for some altered granitoids. Most granitoids are plotted in the high-K series, but the Highland Valley granitoids are least potassic (low-K to med-K). Some Chilean and Erdenet granitoids are most potassic (high-K to shoshonite). The most pertinent feature for the porphyry copper related plutons is highly oxidized nature.

Among the other components, minor and trace elements show regional heterogeneities. $P_2O_5$ is least in the Chilean granitoids. Rb is very low but Sr is highest in the Highland Valley and Medet granitoids. Y, La and Ce are least in the Highland Valley granitoids. Cu is contained erratically but highest in the Chilean granitoids, and also in the Highland Valley granitoids. Mo is the highest in the Erdenet and Highland Valley granitoids. In the Sr/Y diagram, adakite is recognized in all the studied regions, except for Ani mine.

Porphyry copper mineralized granitoids in Chile, Highland Valley, Erdenet, Dexing, and Medet, tend to have high Sr/Y ratios. This mixed occurrences of adakitic and non-adakitic granitoids can be explained by mingling of the adakitic magmas generated by partial melting of warm subducted ocean floor-altered basalts and some sediments, and non-adakitic magma generated by partial melting of gabbroids in the lower crust. The adakites have had high contents of copper and sulfur, because partial melting of such ocean-floor materials were rich in Cu and S. The mingled magmas moved upward; then solidified as a magmatic-hydrothermal plumb-system in the uppermost crust. No adakitic character of the Ani mine stock can be explained by cool subduction slab went down below the NE Japan during the Miocene time.

**Keywords:** Northern Chile, Highland Valley, Erdenet, Dexing, Medet, Ani, granitoids, petrochemistry, adakite

[1] National Institute of Advanced Industrial Science and Technology (AIST)

[2] School of Earth & Environmental Sciences, University of Wollongong, NSW 2522, Australia

[*] Corresponding author: S. ISHIHARA, Central 7, 1-1-1 Higashi, Tsukuba, Ibaraki 305-8567, Japan. Email: s-ishihara@aist.go.jp

## 1. Introduction

Andean plutonisms of Jurassic onward are characterized by oxidized quartz diorite to granodioritic rocks (Ishihara and Ulriksen, 1980). Such rocks are generally considered originated from mafic source rocks existing between the subducting slab and the lower continental crust (Oyarzun, 2000). Under such circumstances, ocean floor materials of both sediments, and fresh and/or altered MORB are subducted and recycled into the island arc magmatism (Nakamura *et al.*, 1985; Ishikawa and Nakamura, 1994), which could be critical to the related metallogeny. Such recycling could be seen in volatiles through sulfur and Li isotopes (Sasaki and Ishihara, 1979; Moriguti and Nakamura, 1998) and also on major silicate phases by partial melting of the subducted slab, which has been called adakite (Drummond and Defant, 1990) or HiSY granitoids for the high Sr/Y ratio (>40; Tulloch and Kimbrough, 2003). The adakitic magmas are considered genetically related to Au and giant Cu porphyries in the Andes (Oyarzun *et al.*, 2001; Martin *et al.*, 2003; Reich *et al.*, 2003), Philippines (Sajona and Maury, 1998), Tibet (Hou *et al.*, 2009) and others. However, genetically related intrusives in a strict sense may not be adakites in the Philippines (Imai, 2002).

Plutonic rocks studied during the Chilean project (Ishihara *et al.*, 1984) were re-examined later years by polarizing XRF method, and some additional samples from other porphyry copper mineralized areas were also analyzed by the same method. In this paper, the authors intend to revisit the works done in northern Chile in the early 1980s (Ishihara *et al.*, 1984), and compared these results to the intrusive rocks from the Highland Valley of southern B.C., Canada, Erdenet mine area in northern Mongolia, Dexing, China, and Medet mine, Bulgaria. Data from the Ani mine stock, which had been high-grade but narrow vein-mineralized in the Japanese Green Tuff Belt, are also added for comparison. The chemical analyses were performed by B. W. Chappell at GEOMOC, Macquarie University, Sydney, Australia. Detailed analytical method was described in Ishihara (2002) and Ishihara and Chappell (2007).

## 2. Mesozoic-Cenozoic granitoids and mineralizations in the southern Peru to the northern Chile

The Mesozoic-Cenozoic granitoids are extensively distributed along the Peru-Chile coast and the Andean Cordillera. The granitoids are divided into the late Paleozoic ilmenite-series and Mesozoic-Cenozoic magnetite-series (Ishihara and Ulriksen, 1980), both of which belong to I-type of Chappell and White (1992). The magnetite-series granitoids intruded into the upper Paleozoic granitoids, and Mesozoic volcanic rocks and sedimentary rocks. The late Paleozoic granitoids, which have magnetic susceptibility of magnetite-free to weakly magnetic values, are only weakly mineralized in the Argentine Andes (Sillitoe, 1977)

In the Peruvian Coast Batholith (Cobbing *et al.*, 1981; Pitcher *et al.*, 1985, eds.), belonging mostly to magnetite-series (Ishihara *et al.*, 2000), the Mesozoic-Cenozoic granitoids are divided into four segments as, Trujillo, Lima, Arequipa and Toquepala, from north to south. These granitoids are of I-type and magnetite-series (Ishihara *et al.*, 2000). Large porphyry copper deposits including Cerro Verde, Cuajone and Toquipala, and some skarn copper deposits are located at the eastern fringe of the southernmost Toquepala segment (Fig. 1). Besides, base metal and Sn and W deposits occur along the inner zone against the batholith, associated with the Cordillera Blanca Batholith (Vidal, 1985).

In the northern Chile, the Mesozoic-Cenozoic granitoids occur as isolated plutons. The older Jurassic granitoids crop out widely along the coast and become younger and smaller bodies in the inland. Thus, deeper levels are exposed to the west but shallower levels toward east. The initial Sr ratios increase eastward from 0.703 to 0.707 (McNutt *et al.*, 1975). The granitoids are mostly quartz diorite to granodiorite in composition, and characterized by high magnetic susceptibility, thus high contents of magnetite, especially toward east (Ishihara and Uliksen, 1980). Predominance of magnetite through the Chilean igneous activities is shown also by Mesozoic magnetite deposits and late Cenozoic magnetite-flow deposits around the El Laco volcanic plug (Henriquez *et al.*, 2003).

Copper is by far most important mineral commodity in the Chilean Andes, occurring as porphyry, manto and vein types (Sillitoe, 1992; Oyarzun, 2000), which are best represented by three major centers from north to south of Eocene-Oligocene Chuquicamata (production +reserves of 66.4 $x10^6$ tons Cu, Table 1), Late Miocene-Pliocene Rio Blanco/Los Bronco (56.7 $x10^6$ tons Cu) and Late Miocene-Pliocene of El Teniente (94.4 $x10^6$ tons Cu) (Camus 2003 in Nakayama 2007). Including smaller deposits, porphyry copper systems are divided into five stages as (A) Cretaceous, (B) Paleocene, (C) Eocene-Oligocene, (D) Early-middle Miocene, and (E) Late Miocene-Pliocene.

These porphyry-type deposits are aligned in three N-S trending belts, namely as the Paleocene-Early Eocene (e.g., Cerro Verde, Cajone, Toquepala, Cerro Colorado; INGEMMET, 2000; Ishihara, 2001), the Late Eocene-Early Oligocene (e.g. El Abra, Chuquicamata, Escondida, El Salvador; Watanabe and Hedenquist, 2001) and the Early-Middle Miocene (e.g., Bajo de la Alumbrera, Rio Blanco, El Teniente; Sillitoe, 1992; Oyarzun, 2000). Molybdenite and native gold are important by-products for the porphyry copper deposits

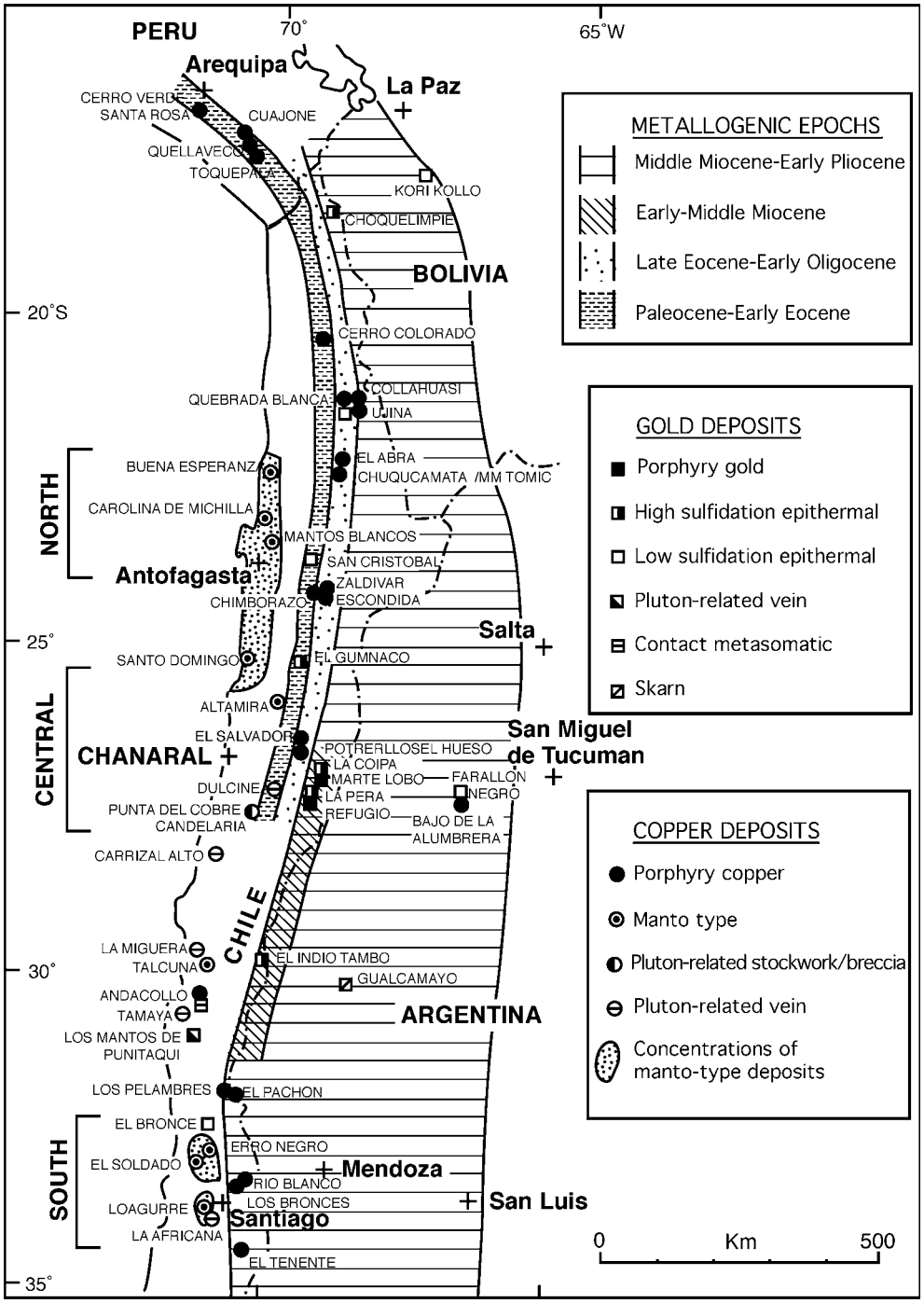


Fig. 1 Distribution of metallic igneous deposits in the northern Chile-Peru (simplified from Sillitoe, 1992) and locations of the studied areas.

(Table 1). Total Mo metal contained in the El Teniente and Chuquicamata deposits are indeed more than that of the Climax Mo deposit.

Other types of ore deposits are hydrothermal breccias, veins, replacement mantos, calcic skarns and manto types related to the Jurassic and Cretaceous mafic and calcic plutonic belts. The vein deposits tend to be hosted in intrusive bodies, whereas the larger composite deposits, such as Candelaria-Punta del Cobre and Mantoverde in the Copiapo region, occur within volcano-sedimentary sequences with some distance from the pluton edge and associated with regional parallel faulting. Some of the composite deposits are recently considered to belong to the iron oxide-copper-gold (IOCG) deposits type (Sillitoe, 2003).

Table 1 Copper, molybdenum and gold contents of Chilean porphyry copper deposits (Camus, 2003 and Nakayama, 2007).

| Ore deposits | Copper | | | | | Molybdenum | | Gold | |
|---|---|---|---|---|---|---|---|---|---|
| | Resource $10^6$ t | Grade Cu% | Contained metal $10^6$ t | Produced metal $10^6$ t | Total amount | Grade Mo % | Contained metal $10^6$ t | Grade Au g/t | Contained metal t |
| ***Cretaceous*** | | | | | | | | | |
| Andacollo | 540 | 0.43 | 2.43 | 0.00 | 2.43 | 0.01 | 0.05 | 0.25 | 135 |
| ***Paleocene*** | | | | | | | | | |
| Cerro Colorado | 194 | 1.00 | 1.94 | 0.57 | 2.51 | 0.015 | 0.029 | 0.000 | 0 |
| Spence | 497 | 0.92 | 4.57 | 0.00 | 4.57 | 0.000 | 0.000 | 0.180 | 89 |
| ***Eocene-Oligocene*** | | | | | | | | | |
| Chuquicamata | 7521 | 0.55 | 41.37 | 25.00 | 66.37 | 0.024 | 1.805 | 0.040 | 301 |
| La Escondida | 2262 | 1.15 | 26.01 | 6.48 | 32.49 | 0.021 | 0.475 | 0.100 | 226 |
| Esperanza | 514 | 0.60 | 3.08 | 0.00 | 3.08 | 0.000 | 0.000 | 0.260 | 134 |
| Gaby Sur | 700 | 0.49 | 3.43 | 0.00 | 3.43 | 0.000 | 0.000 | 0.000 | 0 |
| El Salvador | 974 | 0.63 | 6.14 | 5.15 | 11.29 | 0.022 | 0.214 | 0.100 | 97 |
| Quebrada Blanca | 400 | 0.83 | 3.32 | 0.48 | 3.80 | 0.015 | 0.060 | 0.100 | 40 |
| El Abra | 1544 | 0.55 | 8.49 | 0.85 | 9.34 | 0.005 | 0.077 | 0.000 | 0 |
| Toki | 2411 | 0.45 | 10.85 | 0.00 | 10.85 | 0.000 | 0.000 | 0.000 | 0 |
| Escondida Norte | 1615 | 0.87 | 14.05 | 0.00 | 14.05 | 0.000 | 0.000 | 0.000 | 0 |
| Collahuasi (Rosario) | 3108 | 0.82 | 25.49 | 0.00 | 25.49 | 0.024 | 0.746 | 0.010 | 31 |
| Colahuasi (Ujina) | 636 | 1.06 | 6.74 | 0.94 | 7.68 | 0.000 | 0.000 | 0.000 | 0 |
| Radomiro Tornic | 4970 | 0.39 | 19.38 | 0.55 | 19.93 | 0.015 | 0.746 | 0.000 | 0 |
| ***Early-middle Miocene (Maricunga Belt)*** | | | | | | | | | |
| Refugio (Verde) | 216 | 0.10 | 0.22 | 0.00 | 0.22 | 0.000 | 0.000 | 0.88 | 190 |
| Cerro Casale | 1285 | 0.35 | 4.50 | 0.00 | 4.50 | 0.000 | 0.000 | 0.70 | 900 |
| Lobo | 80 | 0.12 | 0.10 | 0.00 | 1.10 | 0.000 | 0.000 | 1.60 | 128 |
| ***Late Miocene-Pliocene*** | | | | | | | | | |
| Los Pelambres | 4193 | 0.63 | 26.42 | 0.46 | 26.88 | 0.02 | 0.67 | 0.02 | 84 |
| Rio Blanco/Los Broncos | 6991 | 0.75 | 52.43 | 4.30 | 56.73 | 0.02 | 1.26 | 0.04 | 245 |
| El Teniente | 12482 | 0.63 | 78.64 | 15.71 | 94.35 | 0.02 | 2.5 | 0.04 | 437 |
| Total | 53133 | | 340 | 60 | 401 | | 8.632 | | 3037 |

## 3. Magnetic susceptibility and oxidation ratio of the Chilean granitoids

### 3.1. Magnetic susceptibility

I-type magnetite-series rocks of the northern Chile (22°S－34°S) were studied magnetically and chemically in three regions as follows: (1) Varillas-Antofagasta-Tocopilla-Chuquicamata region, which is simply called the North Transect, (2) Ci Funcho-Caldera-Copiapo-El Salvador region, similarly called the Central Transect, and (3) Valparaiso-Santiago-Rio Blanco—El Teniente region, similarly called the South Transect (Fig. 1).

Degree of oxidation can be shown by presence of magnetite, hemoilmenite and hematite in granitoids; but occurrence of hemoilmenite is generally limited. Hematite ($Fe_2O_3$) is unstable in a magmatic temperature; thus magnetite ($Fe_2O_3 \cdot FeO$) is practically indicative for an oxidized magma. Thus, the magnetite contents are useful indicator for oxidized environment, which are easily shown by magnetic susceptibility measurement. The Mesozoic-Cenozoic granitoids of the northern Chile have magnetic susceptibility of the magnetite-series, which is higher than $3.0 \times 10^{-3}$ SI unit (Fig. 2A) or $\chi$-values above $100 \times 10^{-6}$ emu/g (Ishihara *et al.*, 1984). The magnetic susceptibilities are plotted against $SiO_2$ contents in Fig. 2A.

Along the North Transect, the values are negatively correlated with $SiO_2$ contents, and lowest in the Jurassic granitoids and highest in the Tertiary granitoids. Both the Jurassic and Cretaceous granitoids are plotted below the average magnetite-series trend of the Japanese granitoids, but the Tertiary granitoids are located above the average values (Fig. 2A). The Fortuna granodiorite of the Chuquicamata mine area has the highest value (see Appendix 1).

Along the Central Transect, the magnetic susceptibility is again lowest on the older, Jurassic granitoids and higher in the younger, Cretaceous and Tertiary granitoids. Paleogene granitoids of the Copiapo area have the magnetic susceptibility of 26.4-47.6 x $10^{-3}$ SI unit. L porphyry of the El Salvador mine has also a high value of 46.6 x $10^{-3}$ SI unit. This rock contains 0.52 % S (Appendix 1). Because magnetite is the first rock-forming mineral to be converted to iron sulfide when sulfur fugacity increases at the late magmatic stage, the present value seems a minimum

value for this rock.

Along the South Transect, the Mesozoic-Cenozoic granitoids are plotted at just below the average magnetite-series values (Fig. 2A).

### 3.2. Oxidation ratio

Degree of oxidation is directly shown by ferric/ferrous ratio of bulk analyses. $Fe_2O_3$/FeO ratio of 0.5 corresponds empirically to the boundary value between the magnetite-series and ilmenite-series, strictly at $SiO_2$ 70 %. However, the identification using bulk ferric/ferrous ratio is less reliable, because of later alteration, sulfidation of the iron oxides, and also difficulty of the chemical analysis.

Along the North Transect, the Jurassic granitoids having the $Fe_2O_3$/FeO ratio ranging from 0.4 to 0.6, are plotted around the boundary value of the Japanese granitoids (Fig. 2B), but the Cretaceous and Tertiary granitoids have higher ratio, being 0.8—1.7, than the average values (Fig. 2B). The highest value of 3.95 was obtained from the Este porphyry in the Chuquicamata mine area (no. 16, Appendix 1). Thus, the granitoids related to the copper mineralizations appear to be most oxidized.

Along the Central Transect, some Jurassic granitoids (e.g., nos. 20, 22) have very low ratio equivalent to those of the ilmenite-series, while the other ones and Cretaceous and Tertiary granitoids are much oxidized having the ratios higher than 1. Among the rocks from the El Salvador mine, the L porphyry has the highest value as 1.73 (no. 34, Appendix 1), and additional two L porphyries from the drill hole DH1104 are even higher as 3.45 and 5.00 (nos. 35, 36, Appendix 1), which may be due to slight alteration related to weak Mo mineralizations (122, 106 ppm Mo).

Along the South Transect, the Cretaceous granitoids have a lower range as 0.56—1.41 than the Tertiary granitoids that have 0.66 and 1.44. Fine-grained quartz diorites from the depth of the El Teniente mine (nos.46, 47, Appendix 1), containing 1.08 % and 0.49 % S, and 826 and 793 ppm Cu, have much higher $Fe_2O_3$/FeO ratio (more than 3.05). Primary calcium sulfate is commonly seen in the El Teniente deposits. Oxygen fugacity seems to be increased from the magmatic to the post magmatic stages.

## 4. Chemical characteristics of the Chilean granitoids

The chemical compositions studied are listed in

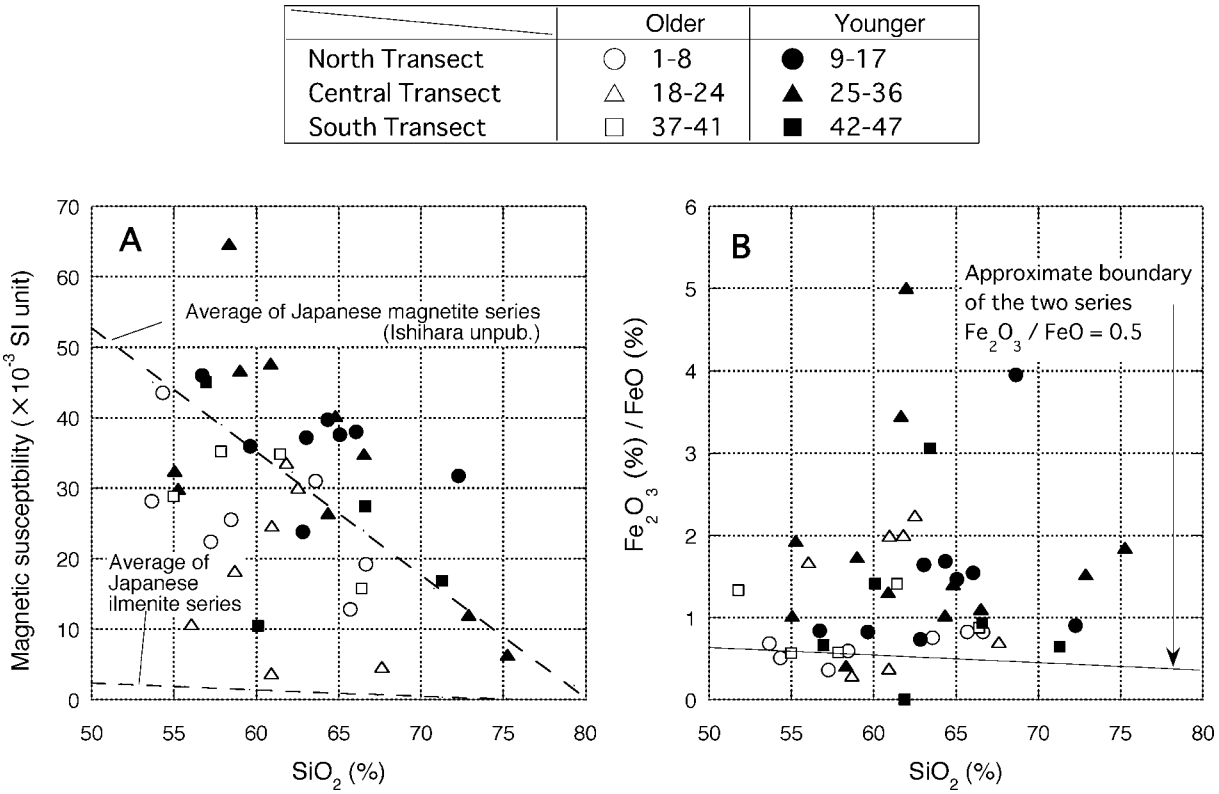


Fig. 2 Magnetic susceptibility (A) and oxidation ratio (B) of the Chilean granitoids across three transects in the northern Chile. Both the data are essentially from Ishihara *et al.* (1984), but magnetic susceptibility converted to SI unit ($x10^{-3}$). Boundary value between the magnetite-series and ilmenite-series is set at 3.0 x $10^{-3}$ SI unit. No. 46 sample is excluded in Fig. 2B for the strong alteration.

Appendix 1. Details of the sample descriptions and the first analytical results by conventional wet methods are given in Geological Survey of Japan (1984) and Ishihara *et al.* (1984). The same powdered samples and some additional samples were re-analyzed by XRF by B. W. Chappell.

Additional samples include unaltered Este porphyry dike from the out side of the Chuquicamata pit (no. 16, Appendix 1) collected by Marcos Zentilli. At the El Salvador mine, two drill core samples of L porphyry (nos. 35, 36, Appendix 1) were selected by Yasushi Watanabe from the DH 1104 (see Fig. 1 of Gustafson and Quiloga, 1995). The samples are weakly mineralized: the S contents are 0.43−0.46 % and Mo contents are 122−106 ppm. Two samples of dacite porphyry were also added from the drill holes of the El Teniente mine (nos. 46, 47, Appendix 1). The rocks have been altered and the magnetite has been converted to hematite and pyrite. Chalcopyrite replaces also magnetite or fills cracks under the microscope. Their S contents of nos. 46 and 46 samples are 1.08 and 0.49 %, respectively, and Cu contents are 826 and 793 ppm, respectively.

Silica contents vary from 48 to 73 %, but generally between 55 and 67 %. That is, gabbroids are present but rare. The studied granitoids from three transects are divided into the coastal side of older, and inland side of younger group, and plotted into selected Harker diagrams (Figs. 3-5). The older groups are Jurassic to Cretaceous in age in the North and Central Transects, but Cretaceous in the South Transect. The younger groups are Cretaceous to Paleogene in the North and Central Transects, but Neogene in the South Transect. These plots are compared with averaged values of the Ryoke granitoids in Japan, which are I-type but ilmenite-series representing the core of the Japanese island arc, and were analyzed by the same analyst as in Chappell and Hine (2006) and Ishihara and Chappell (2007).

**4.1 General characteristics**

$Al_2O_3$ contents are plotted higher than the averaged Ryoke granitoids, which are shown by straight line in Fig. 3, and show good negative correlation with $SiO_2$ content on the younger groups, but some of the older group have low values especially on the low silica range rocks (Fig. 3A). The same tendency is seen on the alumina-saturation index (ASI, Fig. 3B), but the Chilean granitoids are more close to the averaged Ryoke granitoids. The ASI is generally below unity in the Chilean granitoids, which is defined as meta-aluminous and some older granitoids with $SiO_2$ below 60 % have very low ASI of 0.83-0.69. Only two samples of granitic compositions exceed 1.0, i.e., peraluminous (nos. 29, 30, Appendix 1).

It was found that the studied rocks of the older groups in the North and Central Transects, are calcic in the alkali-lime index of Peacock (1931), which is higher than 61, whereas the younger groups in the North Transect are calc-alkalic with the index of 56−61, and alkali-calcic (the index of 51−56) in the younger group of South Transect. It is therefore the plutonism becomes alkalic with younging age (Ishihara *et al.*, 1984). In $K_2O$-$SiO_2$ diagram (Fig. 3C), almost all the studied granitoids of North Transect and Central Transects are plotted in medium K and high K field, and the younger-group rocks are more potassic than the older-group rocks. Along the South Transect, there are two plots in the shoshonite field, which are Cretaceous diorite (No. 39), west of Santiago and Tertiary quartz diorite (No. 43) of SE Santiago. This is considered a local concentration of alkaline in the granitic magmatism.

Strange distribution pattern is seen on $Na_2O$ content (Fig. 3D), because of a large variation in the younger granitoids. For example, the contents go up to 5.7 and 5.8 % at El Salvador and El Teniente with $SiO_2$ 62-64 %, which may have been due to hydrothermal alteration, but is as low as below 2.9 % in the local felsic phase of the granodiorite near Copiapo (Fig. 3D). $Na_2O$-dominant characters are often observed in the magnetite-series granitic terrain (Ishihara and Tani, 2004).

CaO contents are higher in the older group than in the younger group, especially along the North Transect (Fig. 4A). $P_2O_5$ contents show a strange distribution pattern that many of Jurassic-Cretaceous granitoids in the Ci Funcho-Caldera and Copiapo areas of Central Transects, and some of the older group in the Tocopilla area of the North Transect are depleted in the $P_2O_5$ content relative to their $SiO_2$ contents (Fig. 4B). This is commonly seen in hornblende gabbroids in the magnetite-series granitic terrain of the Sanin District in Japan (S. Ishihara, unpublished data), which have had the highest oxygen fugacity during the solidification of the magnetite-series magmas. Most of the other granitoids are, on the other hand, show good negative correlation with $SiO_2$ contents (see Fig. 4B).

Sr contents are low relative to their $SiO_2$ contents in many of the older mafic granitoids of North and Central Transects. The contents are higher than 300 ppm in most of the younger-group granitoids, except for four high $SiO_2$ granites higher than 70 % $SiO_2$ (Fig. 4C). On the other hand, Y contents are higher in the older-group granitoids than the younger group (Fig. 4D). Therefore, high Sr/Y ratios are often observed in the younger granitic terrains in Chile, which are discussed in more details separately. Rb contents are always low and never exceed the amount of Sr, so that the Rb/Sr ratio is always below 0.5 in the Chilean plutonic rocks.

Total iron contents as $Fe_2O_3$ of the Chilean granitoids generally lower than the averaged Ryoke granitoids and show weakly a curved distribution (Fig.

5A). The Chilean granitoids are more dominant in MgO than the averaged Ryoke granitoids (Fig. 5B). This MgO-rich character should be reflection of a primitive character for the Chilean source rocks, as shown by their much lower Sr initial ratio than that of the Ryoke granitoids (Shibata and Ishihara, 1979).

Distribution of V contents against $SiO_2$ is similar to that of $Fe_2O_3$ (Fig. 5C), because the Chilean granitoids belong to magnetite-series and vanadium is mostly contained in rock-forming magnetite. Copper contents, on the other hand, are very sporadic and no relationship with $SiO_2$ and/ or mafic components. The contents are much higher than the Ryoke averaged values (Fig. 5D), which are suggestive for the lack of copper

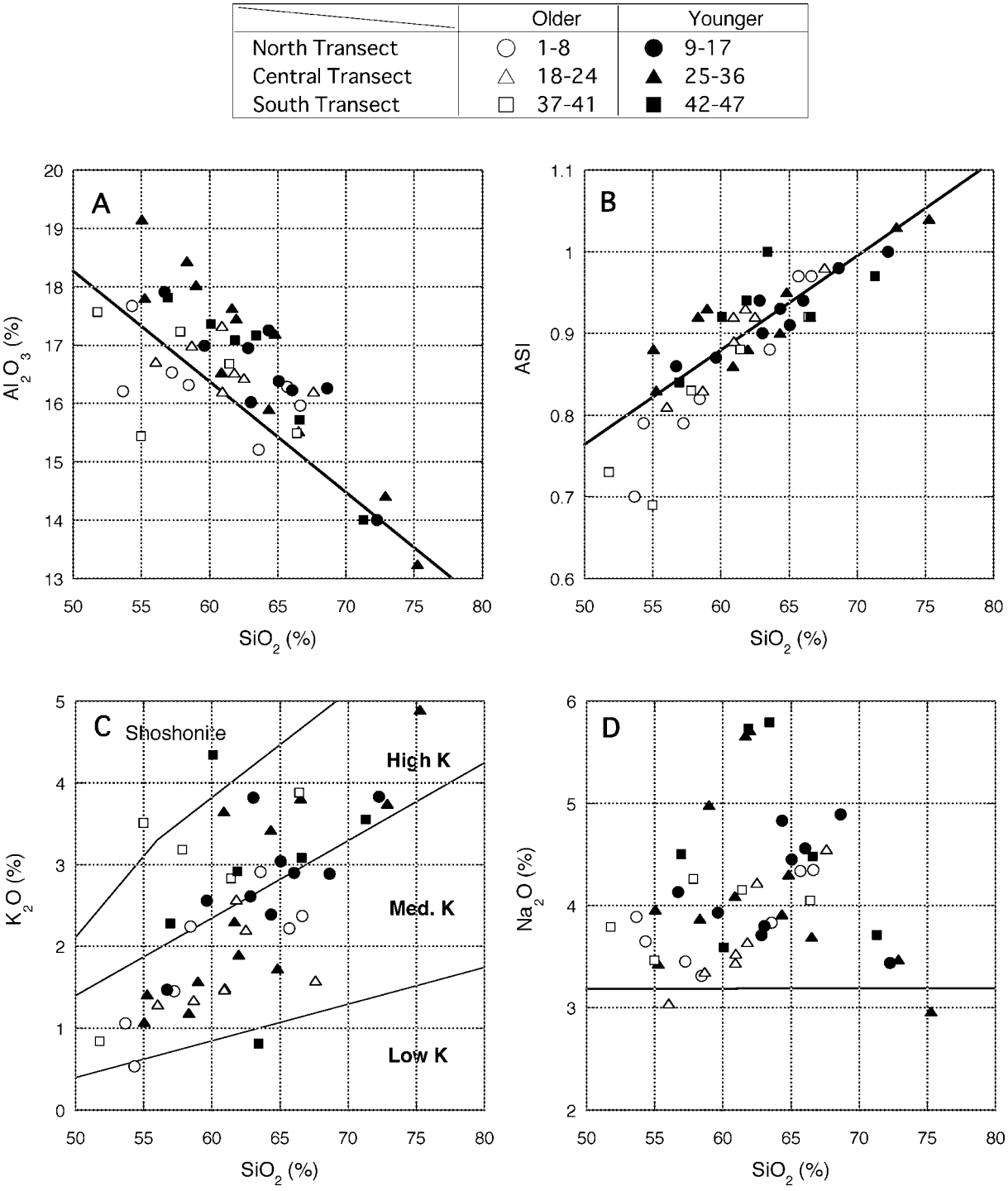


Fig. 3 $Al_2O_3$, ASI, $K_2O$ and $Na_2O$ plotted against $SiO_2$ content of the Meso-Cenozoic granitoids across northern Chile. Thick straight line is averages of the Ryoke ilmenite-series granitoids of Ishihara and Chappell (2007).

mineralizations in the Ryoke Belt.

**4.2 Sr/Y ratio**

High-Sr/Y granitoids occur related to the porphyry copper deposits (Oyarzun *et al.*, 2001). In the North Transect (Fig. 6A), both Jurassic and Cretaceous granitoids are identified low in the Sr/Y ratio. The Y contents are grouped into low (9-12 ppm, nos. 2-4, Appendix 1) and high groups (more than 18 ppm, nos. 1, 5-8, Appendix 1). The Cretaceous granitoids of the Andina granodiorite (nos. 9, 10, Appendix 1) are similar to the high group.

Tertiary granitoids in further east of the Chuquicamata mine area are composed of several

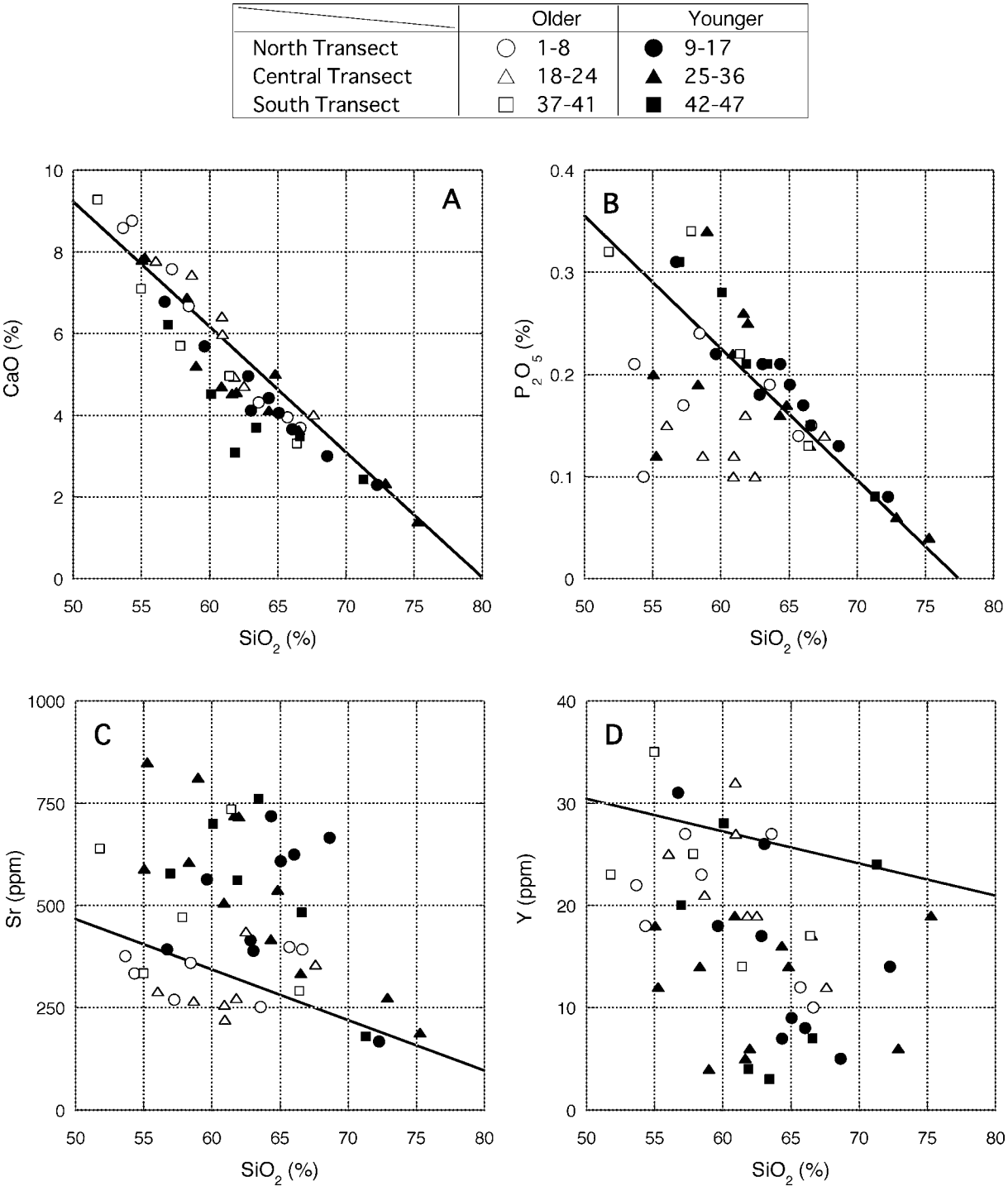


Fig. 4 CaO, $P_2O_5$, Sr and Y plotted against $SiO_2$ content of the Meso-Cenozoic granitoids in the northern Chile. Thick straight line is averages of the Ryoke ilmenite-series granitoids of Ishihara and Chappell (2007).

intrusive phases (Ossandon *et al.*, 2001). The Eocene-Oligocene Fortuna granodiorite from the southwest of the open pit (nos. 12, 13, Appendix 1) and the western flank of the pit (no. 11, Appendix 1) are very high in Sr ratio and low in Y content, thus typically high-Sr/Y granodiorite. The Este porphyry from the Chuquicamata pit has the highest Sr/Y ratio of 133 (no. 16, Appendix 1). Tonalite and granodiorite from the north of the Chuquicamata mine area are, however, not high in the Sr/Y ratio (nos. 14, 15, Appendix 1).

In the Central Transect (Fig. 6B), Sr/Y ratio is low with high Y content in the Jurassic granitoids of the coastal Chanaral area (nos. 18-23, Appendix 1), The Cretaceous granitoids are generally high in the Sr/

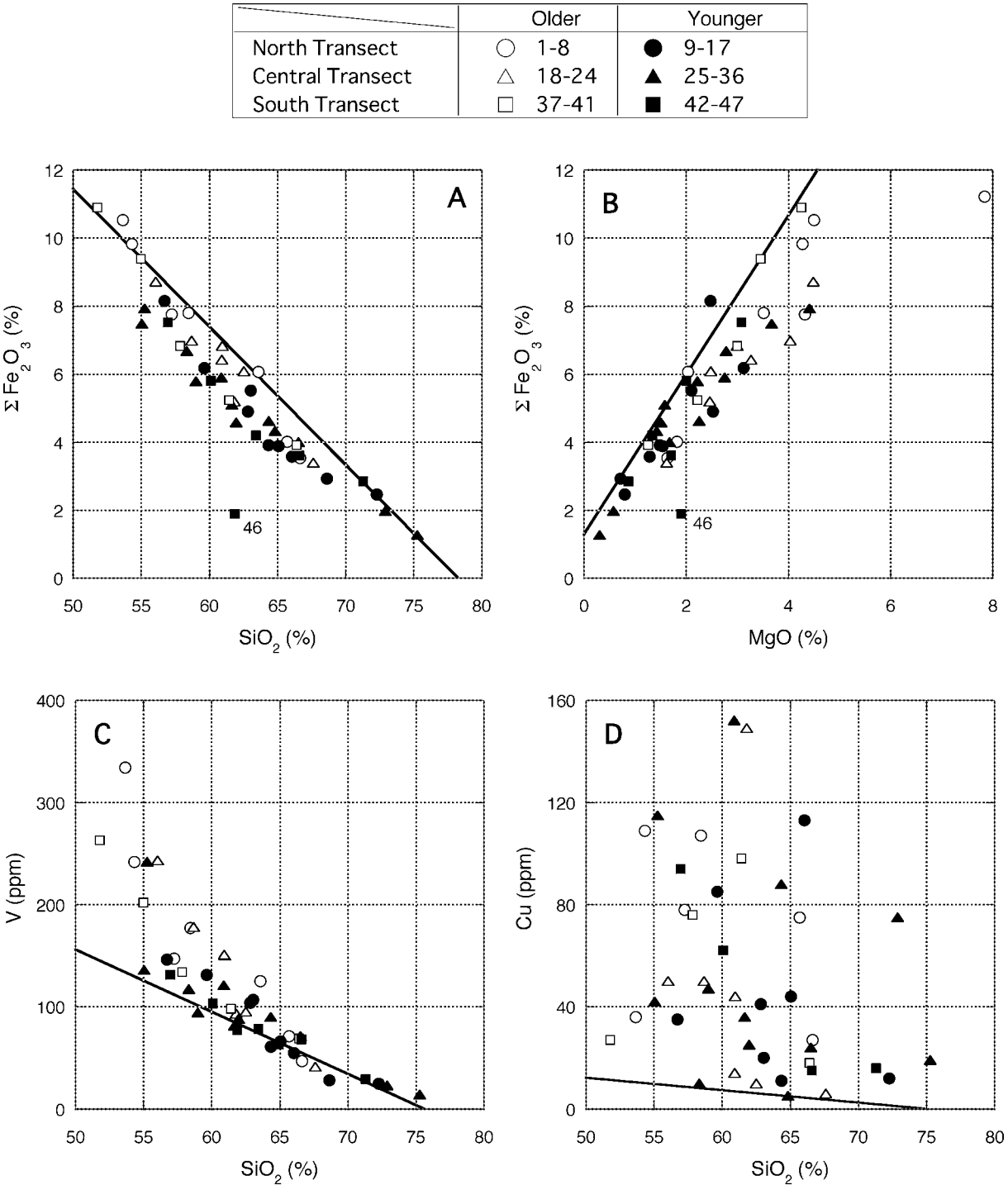


Fig. 5 $Fe_2O_3$, V and Cu plotted against $SiO_2$ content and $Fe_2O_3$-MgO diagram of the northern Chilean granitoids. Thick straight line is averages of the Ryoke ilmenite-series granitoids of Ishihara and Chappell (2007).

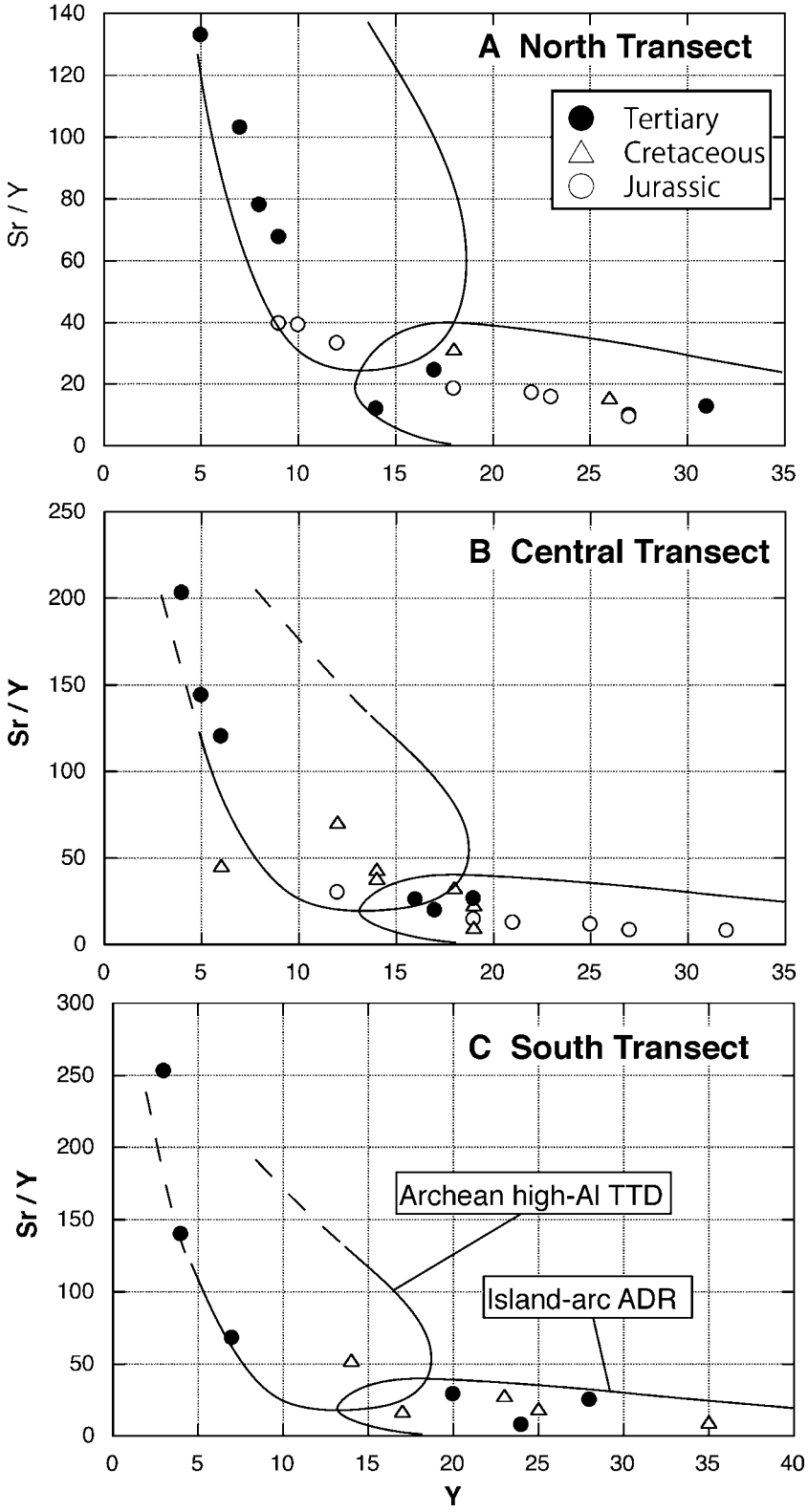


Fig. 6 Sr/Y ratio vs. Y content of the studied granitoids in the northern Chile. Circled areas for Archean high-Al TTD (trondhjemite-tonalite-dacite) and Island-arc ADR (andesite-dacite-rhyolite) from Tsuchiya and Kanisawa (1994).

Y ratio because of lowering the Y content, thus four samples (nos. 25, 27-29, Appendix 1) are plotted in the high-Sr/Y field. Tertiary granitoids of the Copiapo area (nos. 31-33) are not high in the Sr/Y ratio (nos. 34-36, Appendix 1), as pointed out by Oyarzun *et al.* (2001).

In the South Transect, almost all the Cretaceous granitoids have low-Sr/Y ratio, except for Cretaceous tonalite from the west of Santiago (no. 41, Appendix 1). The Tertiary granitoids are also non-adakitic in general, except for the porphyry Cu-mineralized area. The granodiorite (4 Ma) from the Rio Blanco porphyry copper deposit (no. 45, Appendix 1) and fine-grained quartz diorite which has been mineralized in the depth of the El Teniente porphyry copper deposits (nos. 46, 47, Appendix 1) is strongly high in the Sr/Y ratio.

In summary, the high-Sr/Y granitoids have not been observed in the Jurassic granitoids in the coastal Chile and in most of the Cretaceous granitoids of the interior across the Antofagasta, Copiapo and Santiago transects. High-Sr/Y characters are most distinct in the Tertiary granitoids; thus, there is a tendency that the Chilean magmatism becomes high-Sr/Y with younging ages. Those related to the major porphyry copper deposits, such as, Fortuna granodiorite and Este porphyry at Chuquicamata, L porphyry at El Salvador, and granodiorite-quartz diorite at Rio Blanco and El Teniente, are always high in the Sr/Y ratio.

## 5. Other porphyry-Cu mineralized regions

Granitoids collected during short visits associated with scientific meetings are analyzed and reported here. These include Highland Valley region of southern B.C., Canada, Erdenet mine of Mongolia, Dexing mine of southern China, Medet mine of Bulgaria, and Ani mine in Japan. All are Mesozoic to Cenozoic in age. The analytical results are given in Appendices 2 and 3.

### 5.1 Highland Valley, B.C., Canada

Granitoids of the Highland Valley mineralized region belong to arc-related magmatism of North American Cordillera (Mortimer, 1986). Five major porphyry copper-molybdenum deposits, Valley, Lornex, Bethlehem, Highmount and JA, are known to occur within 15 $km^2$ in the Highland Valley of the central part of the late upper Triassic (210 Ma), Guichon Creek batholith. The batholith is composed of I-type magnetite-series (Ishihara, 1971; Casselman *et al.*, 1995).

Various intrusive phases of quartz diorite to granodiorite are known. Almost all the sulfide mineralizations in Highland Valley deposits occur in fractures, veins, faults or breccias. Fracture density is the most important single factor influencing ore grades. The mineralization ages range from 202 to 192 Ma (Casselman *et al.*, 1995). Remaining minable reserves on January 1, 1994 were 508 MT at 0.44 % Cu and 0.006 % Mo in the Valley (formally with Copper), and 119 MT at 0.36 % Cu and 0.013 % Mo in the Lornex deposits (Casselman *et al.*, 1995).

The studied specimens were collected mainly from the Jergy pit and Lornex areas, which are described in Ishihara (1971). They have silica range of 61.0 to 70.9 %, and magnetic susceptibility ranging from 13 to 46 x $10^{-3}$ SI unit, except one strongly mineralized rock (e.g., 68BE04, Appendix 2). The bulk $Fe_2O_3/FeO$ ratio varies from 0.53 to 1.12 (Ishihara, 1971). Therefore, they belong to I-type magnetite-series. $K_2O$ contents are rather low, varying from 0.55 to 2.79 %.

### 5.2 Erdenet, Mongolia

Erdenet porphyry copper deposits of northern Mongolia have been mined since 1978. The ore reserves in 1991 were said to be 1,490 MT with 0.509 % Cu and 0.015 % Mo, which contain 7.6 MT copper and 216,600 ton molybdenum metals (Gerel and Munkhtsengel, 2005). The Erdenet mine is located within the Paleozoic Orkhon-Selenge Trough at south of the Siberian Craton. Therefore, the mine area is underlain by Neoproterozoic to Paleozoic basement, Permian Khani Group of felsic to mafic volcanic rocks, and Permian Selenge intrusive complex, which are covered by and intruded by Triassic volcanic and intrusive rocks.

Within the mine site, the Selenge intrusive complex is intruded by various early Mesozoic Erdenet intrusions, including porphyritic granodiorite, dacite partly brecciated, granodiorite porphyry and plagio-porphyry, which host Cu- and Mo-mineralizations. The related alterations from the core to the periphery of the ore deposits, are quartz-sericite, intermediate argillic (chlorite-sericite) and propylitic (chlorite＞epidote).

Gerel and Munkhtsengel (2005) reported silica contents of 50.2 to 74.4 % for the Selenge granitic complex (n＝8), and $Fe_2O_3/FeO$ ratio of 0.6 to 1.4, except one low value of 0.3. Therefore, the complex belongs mostly to I-type magnetite-series. For the Erdenet group of plutonic rocks, they reported 49.9-71.2 % $SiO_2$ (n＝7) and $Fe_2O_3/FeO$ ratio of 1.6 to 0.5 (n＝5). Hence, they belong to I-type magnetite-series. Naito *et al.* (1996) showed a sharp peak at 71 % $SiO_2$ after analyzing many Erdenet granitoids, and pointed out that the Erdenet group of plutonic rocks are more silicic than the Selenge intrusive complex.

We studied least altered granitoids of three samples from pit area, and three samples from the Naito's collection. These rocks show silica range of 55.3-72.7 %, and $K_2O$ content of 1.1 to 4.8 %, except one sodic granite (7.1 % $Na_2O$, Er76, Appendix 2). These least altered rocks reveal magnetic susceptibility from 23.0 to 33.6 x $10^{-3}$ SI unit in general, thus they are strongly magnetite bearing formed under oxidized environment.

**5.3 Dexing, China**

Dexing porphyry copper deposits are situated in the northern part of South China, close to the boundary between the Yangtze Block and Cathaysia Block. The area is underlain by late Proterozoic metamorphic rocks of sandstone and siltstone origin, which are cross-cut by northwest-trending granitic cupolas of the early Yanshanian intrusion, called Zhushahong, Tongchang and Fujiawu from NW to SE. All are mineralized, but the Tongchang is the largest having a total ore reserves of 9.6 MT copper at 0.42-0.50 % Cu and 0.01-0.02 % Mo. The ore deposits are considered to have formed by post-magmatic hydrothermal activities of adakitic magmas generated by partial melting of delaminated lower crust (Wang *et al.*, 2006).

The studied sample is magnetite-bearing hornblende-biotite granodiorite from exploration drill core given in the June visit of 1979. It has a high $Fe_2O_3$/FeO ratio of 0.90, belonging to magnetite-series granitoids.

**5.4 Medet mine, Bulgaria**

There is a strongly mineralized volcano-plutonic arc in the Balkans-South Carpathians, which could have been generated either northward subduction of the Tethian oceanic crust, or break-off of the subducted lithosphere. The magmatism initiated at 92.1 Ma K-Ar age and finished at 76 Ma K-Ar age near the border to the Rhodopes. The low $^{87}Sr/^{86}Sr$ ratios of 0.704 to 0.706 (Kamenov *et al.*, 2007) indicates a juvenile crust source or mantle source with some modification of crustal materials. Re-Os ages of mineralized molybdenites showed the oldest age, 87-92 Ma, in the largest Srednogorie zone, then 81-88 Ma and 72-83 Ma to the northwest and northwards toward the Tomok and Apusent-Banat Zone (Zimmerman *et al.*, 2008).

Three porphyry types including the Medet deposits are located in the Panagyurishte region, just east of the capital Sofia, and the following production and reserves were reported (Popov *et al.*, 2003):

(1) Medet, mined in 1964-1979: 163 Mt at 0.32 % Cu (522, 000 tons Cu), and 0.1 g/t Au (16.3 t Au).
(2) Assarel, mined since 1976: 100 Mt at 0.53 % Cu, trace Au.
Remaing resource: 254 Mt at 0.41 % Cu.
(3) Elatsite, mined since 1981: 165 Mt at 0.38 % Cu, 0.21 g/t Au.
Remaining resource: 154 Mt at 0.33 % Cu.

Medet porphyry copper deposits, located in the intermediate to felsic magmatic arc, occur in small-scale stock (～3 $km^2$), which can be a bigger mass at depth shown by huge magnetic anomalies observed. The stock, having zircon U-Pb age of 89.6-90.4 Ma and K-Ar age of 90-88 Ma, is composed of (i) quartz-monzodiorite, equigranular and rarely porphyritic, (ii) granodiorite, and (iii) dike and small mass of quartz monzodioritic, granodioritic, and quartz monzonitic porphyries. These granitoids are plotted in high-K series in the $K_2O$-$SiO_2$ diagram (Kamenov *et al.*, 2007).

The studied samples were collected from the open pit during the IAGOD field excursion in October, 1974. Their silica contents vary from 56.8 to 69.2 % with $K_2O$ contents of 2.4 to 4.3 %, which are plotted in the high-K series. These granitoids are strongly magnetic having the magnetic susceptibility between 27.6 and 40.4 x $10^{-3}$ SI unit and $Fe_2O_3$/FeO ratio of 0.9 to 1.15 (Appendix 2).

**5.5 Ani mine, Japan**

Japanese islands arc is notorious for not having any porphyry copper deposits. But one that is most close to that type may be vein-type deposits associated with small Miocene quartz dioritic to granodioritic bodies of the Ani mine in the Green Tuff region. Many narrow but high-grade veins are scattered in an area with N-S 7 km and E-W 6 km in Miocene volcanic rocks and also in the quartz diorite- granodiorite intrusion; all mined out by underground working for each high-grade vein. If this deposit would have discovered in recent years, open-pit bulk mining may have been considered.

The mining of the ore deposits was initiated to collect placer gold in 1309, then silver veins were found in 1387 and started their production in 1597, and later the mine became copper and some lead producer. Since the mining is too old, it is not possible to figure out the total production. A good speculation may be ca. 100,000 tons Cu metal and 3 tons Au plus placer gold. Silver and lead were also recovered in small amounts after World War II (Japan Mining Association, 1968).

The mine area is underlain by various volcanic sequence of Miocene age, ranging in composition from basalt to rhyolite (Fig. 7). They are folded and intruded by very small intrusions with quartz dioritic to granodioritic composition, which have volcanic looking chilled margin. They are distributed in 1.5 by 4.0 km at the Taisho Adit level, and exposed partly on surface. Mineralized fractures are grouped in N-S, NE and E-W trends with steep dips (Kamiyama *et al.*, 1958). Good ore veins tend to occur in the intrusive granitoids and also in the footwall dolerites. The veins are narrow but high grade composed mainly chalcopyrite and pyrite associated with galena, sphalerite and native gold, together with quartz, chlorite, hematite and rare sericite, barite and calcite. Vein adularia gives a Miocene K-Ar age of 11 Ma (Yamaoka and Ueda, 1974).

Magnetic susceptibility of these rocks are generally as high as 10.3-46.2 x $10^{-3}$ SI, because they belong to magnetite-series and are mafic in composition, a quartz diorite to granodiorite. Their $Fe_2O_3$/FeO ratios are also high as 0.8-1.1 (Appendix 3).

## 6. Petrochemistry of granitoids in the other regions

Analyzed chemical data from five studied region, other than Chile, are listed in Appendices 2 and 3, and plotted in the Harker's diagrams from Figs. 8 to 13 except for rather severely altered and mineralized rocks of 68BE04 (Highland Valley), ER03 (Erdenet) and 71AN18 and 19 (Ani mine).

ASI, alumina saturation index, is below 1.1 (Fig. 8A), in general, indicating all the rocks belong to I-type. Among the studied granitoids, ASI of the Ani mine stock is highest, having the values between 1.0 and 1.1, which is unclear on the $Al_2O_3$- $SiO_2$ diagram (Fig. 8B). ASI of the Highland Valley area, southern B. C. and Erdenet mine are similar to the values of Chilean granitoids (Fig. 8A). Granodiorite of Dexing mine has one of the lowest values of 0.82 at 62.9 % $SiO_2$

CaO contents are very low in the Ani mine stock, whereas the other rocks are plotted similarly to those of the Chilean granitoids (Fig. 8C). $P_2O_5$ contents of the studied granitoids are negatively correlated with that of $SiO_2$ contents (Fig. 8D). The Chilean granitoids are strange having low $P_2O_5$ contents at the low silica range, which are characteristic of magnetite-bearing gabbroids in the Izumo District in Japan (Ishihara and Chappell, 2008), where the oxygen fugacity during the crystallization is the highest and their rock-forming magnetite has been mined from the weathered crust for more than 1,000 years of history.

In $K_2O$-$SiO_2$ diagram (Fig. 9A), the porphyry copper-related granitoids are mostly plotted in the high-K and medium-K fields, among which those of the Highland Valley are the lowest, plotted in the low to medium-K fields. The Erdenet rocks are plotted in the medium to high-K field, similarly to the Chilean granitoids. The Dexing stock is plotted in the high K, including data by Wang *et al.* (2006).

Reflecting these $K_2O$ contents, Rb is most depleted in the Highland Valley granitoids. Rb contents of the other regions are plotted similarly to the Chilean granitoids (Fig. 9B). Among other feldspar components, Ba has wider variations than those of the Chilean granitoids (Fig. 9C). The Ani mine and Dexing stocks are particularly predominant in Ba. Except for the Ani mine stock, Sr contents are high in most of the granitoids (Fig. 9D), which will be discussed later together with their Y contents.

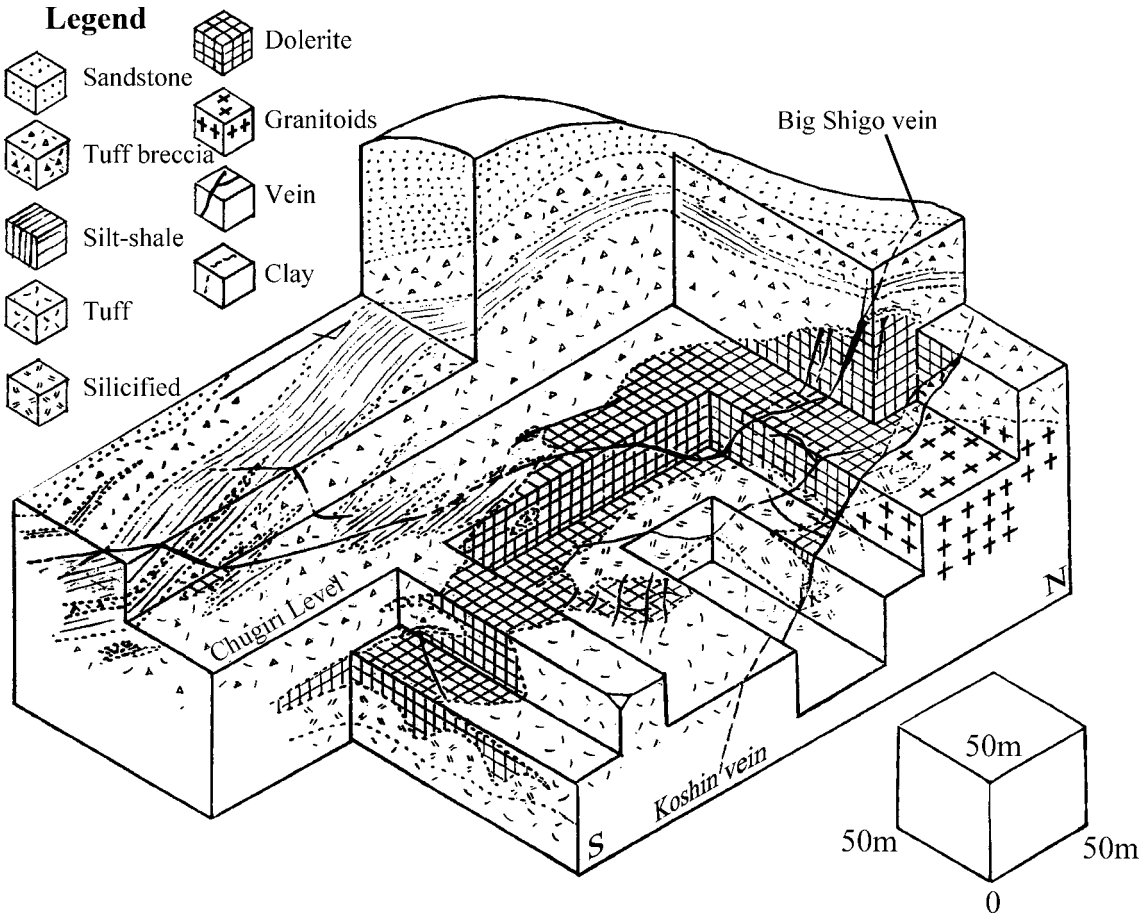


Fig. 7 Block diagram of the central part of Ani copper mine (after Kamiyama *et al.*, 1958).

$TiO_2$ contents of the granitoids in the other regions follow generally distribution trends of the Chilean granitoids, but are slightly higher in those of Erdenet and Ani mines stocks (Fig. 10A). On the other hand, those of the Highland Valley area and Medet mine stock are lower than those of the Chilean granitoids. MgO contents are similar between the Chile and the other regions. Total $Fe_2O_3$ contents are also similar, but are less in the Highland Valley area and higher in the Ani mine stock. The same tendencies are also seen in the MnO contents.

Y contents are generally high in the Chilean granitoids and Ani mine stock, and least in the Highland Valley granitoids. Light rare earth elements (LREE) of La (Fig. 11B) and Ce (Fig. 11C) are also depleted in the Highland Valley granitoids. Vanadium (Fig. 11D), which may be substituted in rock-forming magnetite, shows good negative correlation with $SiO_2$ content and

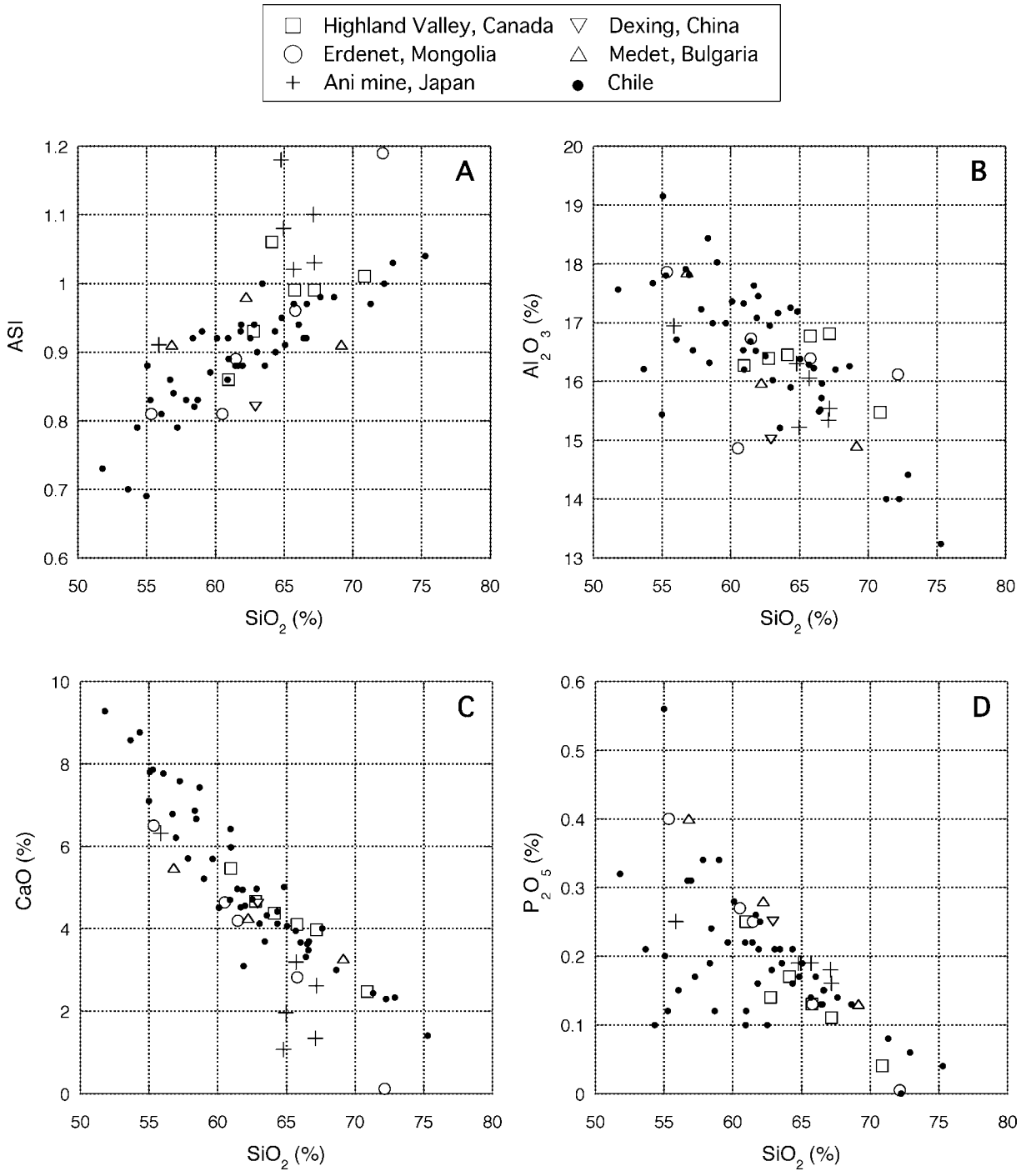


Fig. 8 Comparison of ASI, $Al_2O_3$, CaO and $P_2O_5$ contents between the Chilean and other mineralized granitoids.

positive correlation with $Fe_2O_3$.

Both Ni and Zn contents (Figs. 12A and C) show broadly negative correlation with silica contents, indicating both the elements are substituting FeO of mafic silicates. The Ani mine stock is rich in Zn, as compared with the Chilean and other granitoids. Copper contents are very high, often over 20 ppm, which are contrasting less 20 ppm Cu of orogenic un-mineralized granitoids (55-78 % $SiO_2$) of the Ryoke Belt in Japan. Pb contents should follow $K_2O$ thus $SiO_2$ contents but erratic in Fig. 12D, because of high values on the Ani mine stock and some Chilean granitoids.

Ga content (Fig. 13A), a good indicator of anorogenic A-type granitoids, is generally low, below 21 ppm, implying that the studied granitoids are orogenic type. Zr contents are high in the Ani mine stock and Erdenet rocks, but very low in the Highland Valley granitoids (Fig. 13 B). Distribution trends of

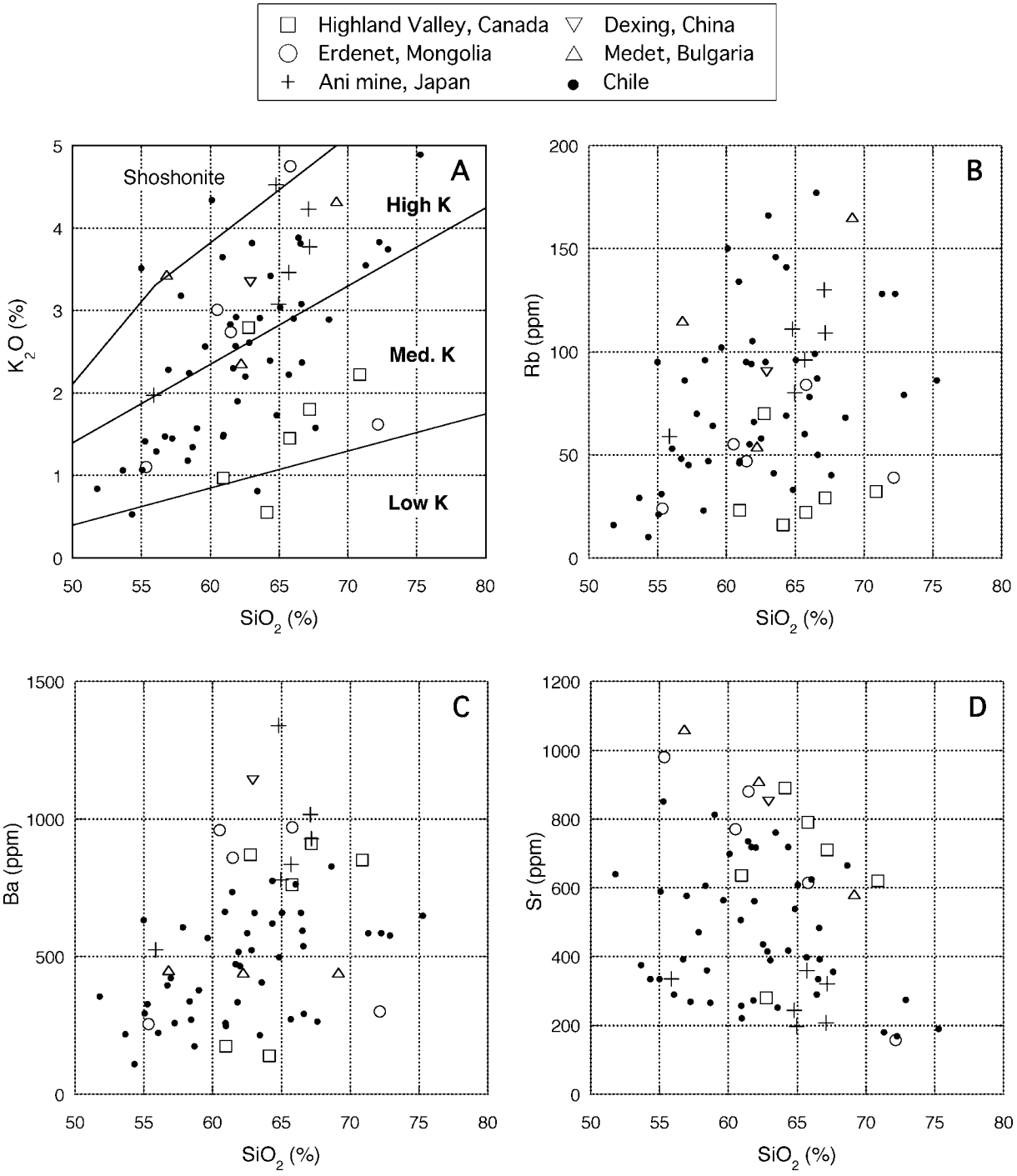


Fig. 9 Comparison of $K_2O$, Rb, Ba and Sr contents between the Chilean and other mineralized granitoids.

the Chilean and Erdenet granitoids have those of high-temperature I-type of Chappell *et al.* (1998).

Sn contents are very low, below 3 ppm (Fig. 13C). The values are surprisingly low compared with ilmenite-series tin granites. The Cornubian granites of Southwest England, a classic tin-mineralized region, have a range of 8-78 ppm (Chappell and Hine, 2006). Mo contents, on the other hand, are much higher than the Ryoke orogenic granitoids containing 0.3 to 3 ppm Mo (Ishihara and Chappell, 2007), especially on the Erdenet and Highland Valley granitoids (Fig. 13D). The Mo contents are not highest in the high $SiO_2$ range but around 60-65 % $SiO_2$ (Fig. 13D).

## 7. Some pertinent features and genetic discussion of the related intrusives

As described in the previous chapters, the

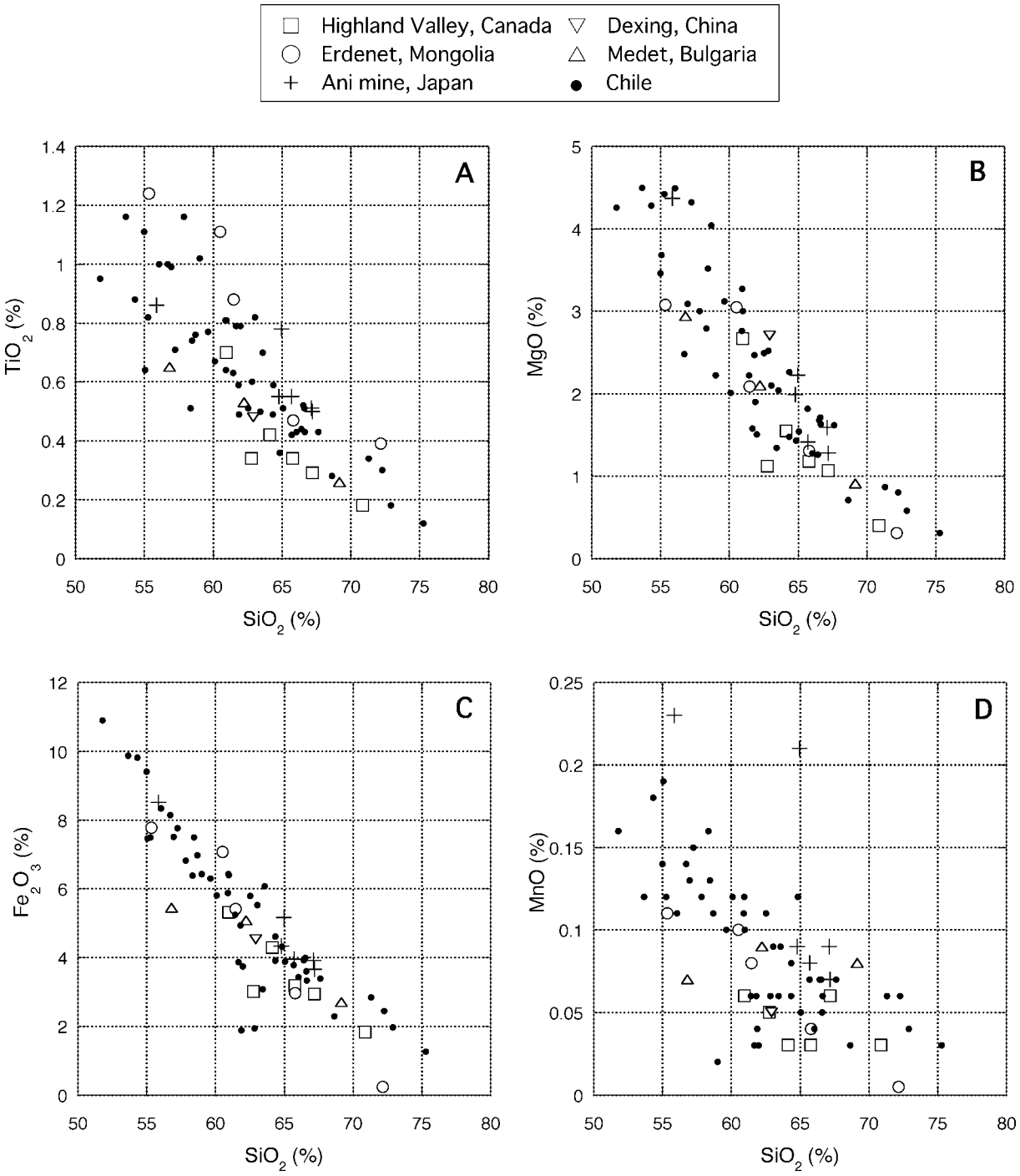


Fig. 10 Comparison of $TiO_2$, MgO, $Fe_2O_3$ and MnO contents between the Chilean and other mineralized granitoids.

most common feature of the intrusive rocks related to porphyry copper deposits are high in magnetic susceptibility belonging to magnetite-series, high in $Fe_2O_3/FeO$ ratio, thus high in the oxygen fugacity during the solidification of the granitic magmas. In the classic alkali classification, the related granitoids belong generally to medium-K and high-K series, but some Au-rich porphyry copper deposits are associated with shoshonite (Muller *et al.*, 1994; Miller and Groves, 1995). They are not per-aluminous but meta-aluminous; therefore no S-type granitoids in the porphyry copper regions. A-type granitoids with low to moderate oxygen fugacity (Loiselle and Wones, 1979) are also different type of granitoids from those related to porphyry Cu-mineralizations. Accordingly, highly oxidized granitic magmas are only pertinent to the porphyry copper mineralizations.

Recently adakitic intrusions with high Sr/Y ratio

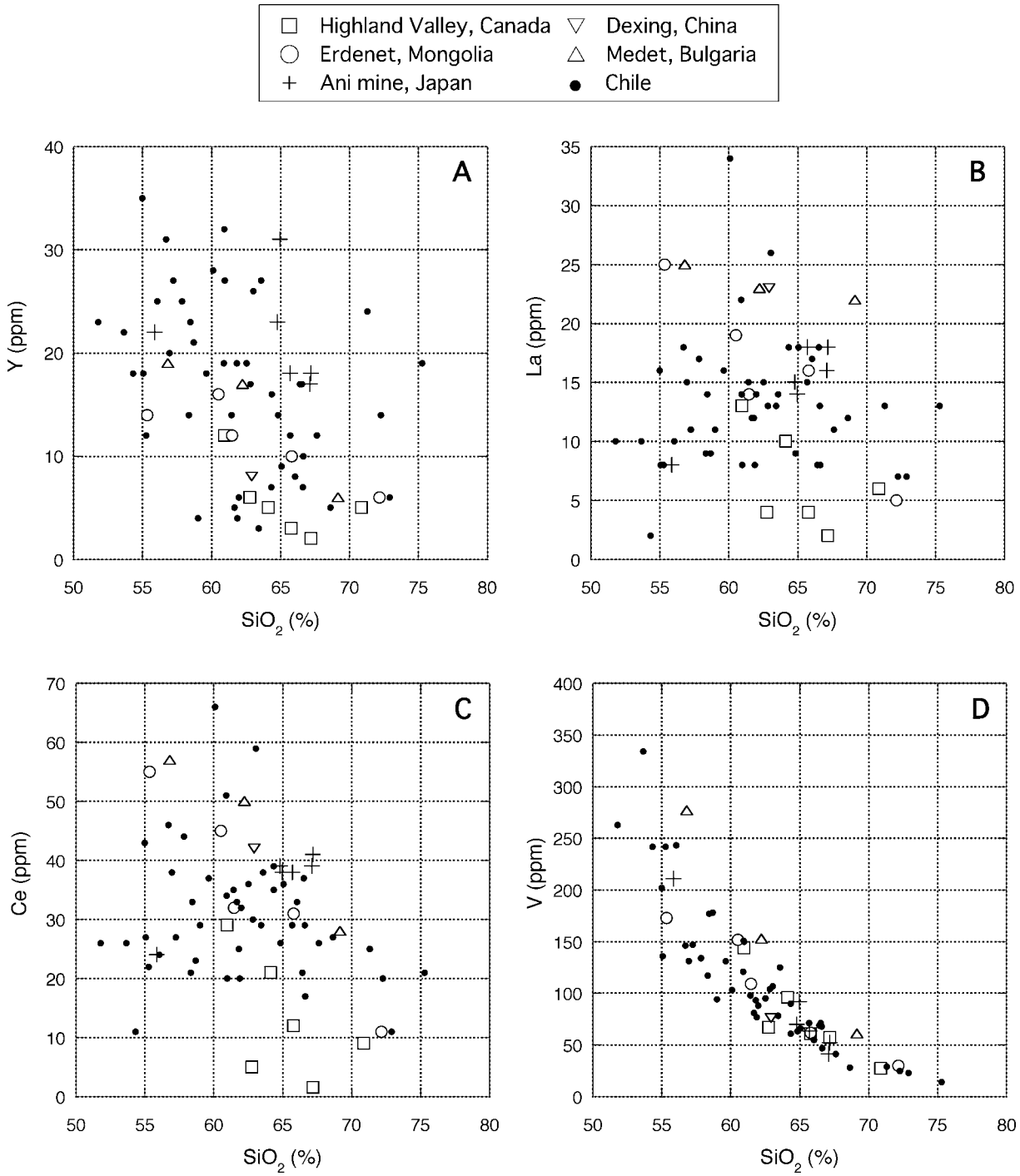


Fig. 11 Comparison of Y, La, Ce and V contents between the Chilean and other mineralized granitoids.

(＞20-40; Drummond and Defant, 1990) have often reported from many porphyry copper regions in Chile, Philippines, China and elsewhere. Here, adakitic granitoids occur in the intrusives from the southern B.C., Erdenet, Dexing, and Medet, besides Chile (Fig. 14). Therefore, adakites should have genetic implication for the formation of porphyry copper deposits. The adakites are most typically generated by partial melting of warm subducting oceanic slab, which may have had hydrothermal alteration at the oceanic ridge. Mafic volcanic rocks are rich in trace amounts of copper, and the sea floor alteration may increase S content in the basalts. Such altered oceanic basalt could be a good starting material for the porphyry copper-related magmas.

Porphyry copper mineralization is a huge magmatic-hydrothermal convection system developed around the top of intrusive bodies, concentrating large amounts

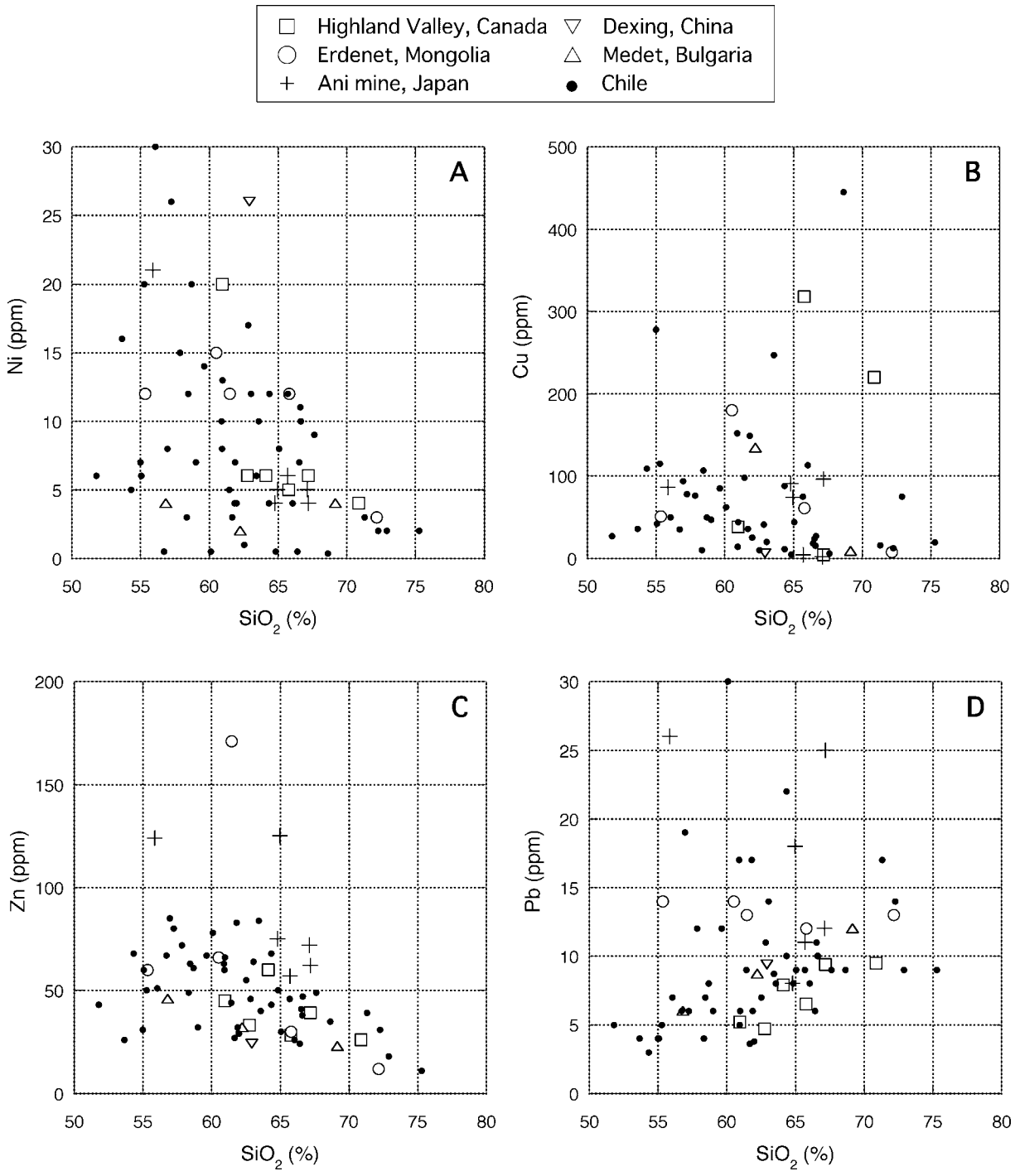


Fig. 12 Comparison of Ni, Cu, Zn and Pb contents between the Chilean and other mineralized granitoids.

of copper and sulfur there. Fig. 15 shows Cu and S contents of the altered and mineralized granitoids in the Erdenet pit. They altogether have a good positive correlation, indicating that both copper and sulfur were brought up together and convected by hydrothermal solution. These anomalous amounts of copper and sulfur must have been originated in the host granitoids.

In Chile, Jurassic to Tertiary granitoids have the following high averaged values of copper:

*North Transect:* Jurassic: 87 ppm Cu (n=8);
Cretaceous-Tertiary Chuquicamata area: 96 ppm Cu (n=8).
*Central Transect:* Jurassic 52 ppm Cu (n=6);
Cretaceous 39 ppm Cu (n=7) and Tertiary 62 ppm (n=6).
*South Transect:* Cretaceous 99 ppm Cu (n=5),
Tertiary 301 ppm Cu (n=6).

These values are much higher than averaged values

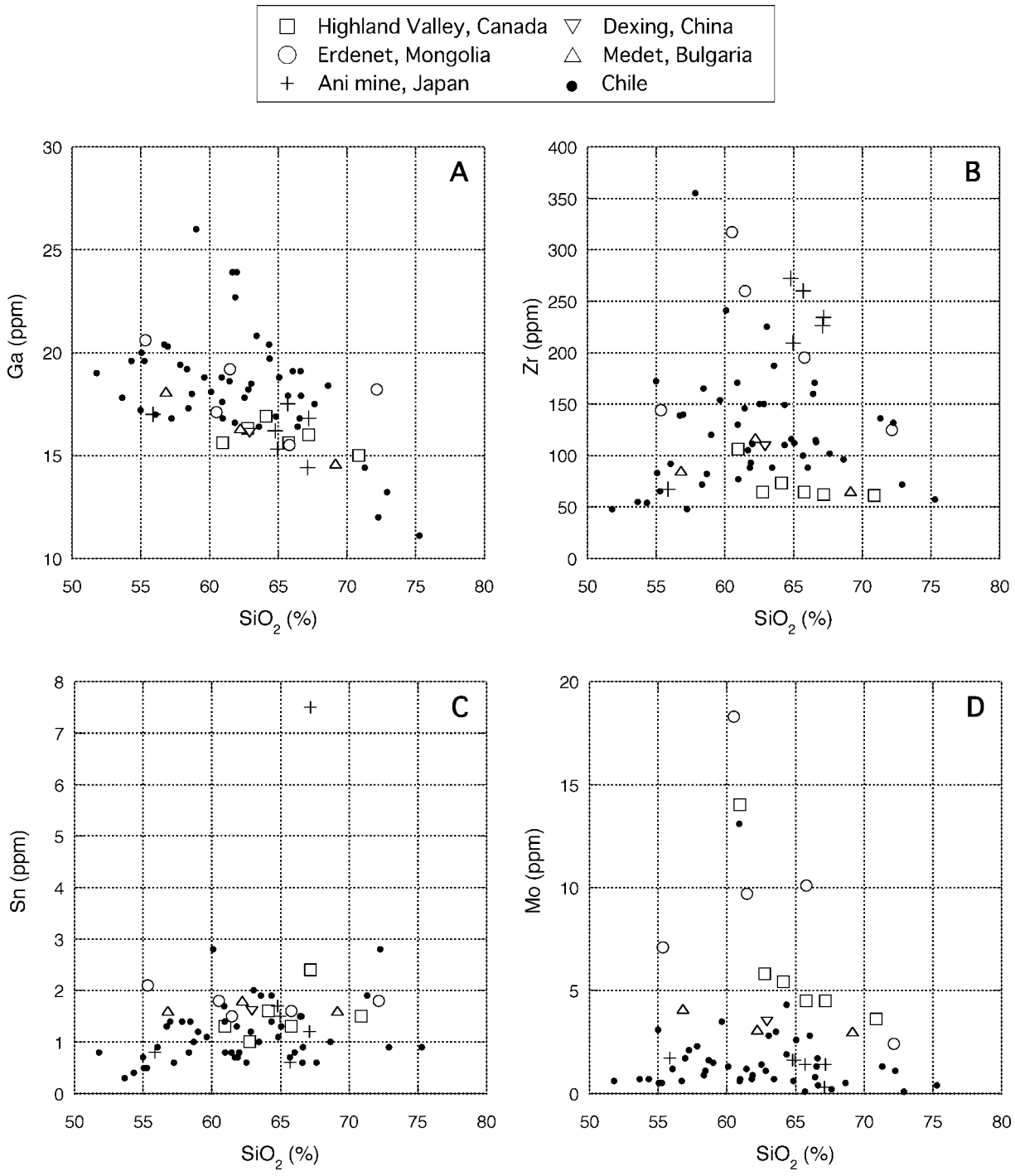


Fig. 13 Comparison of Ga, Zr, Sn and Mo contents between the Chilean and other mineralized granitoids

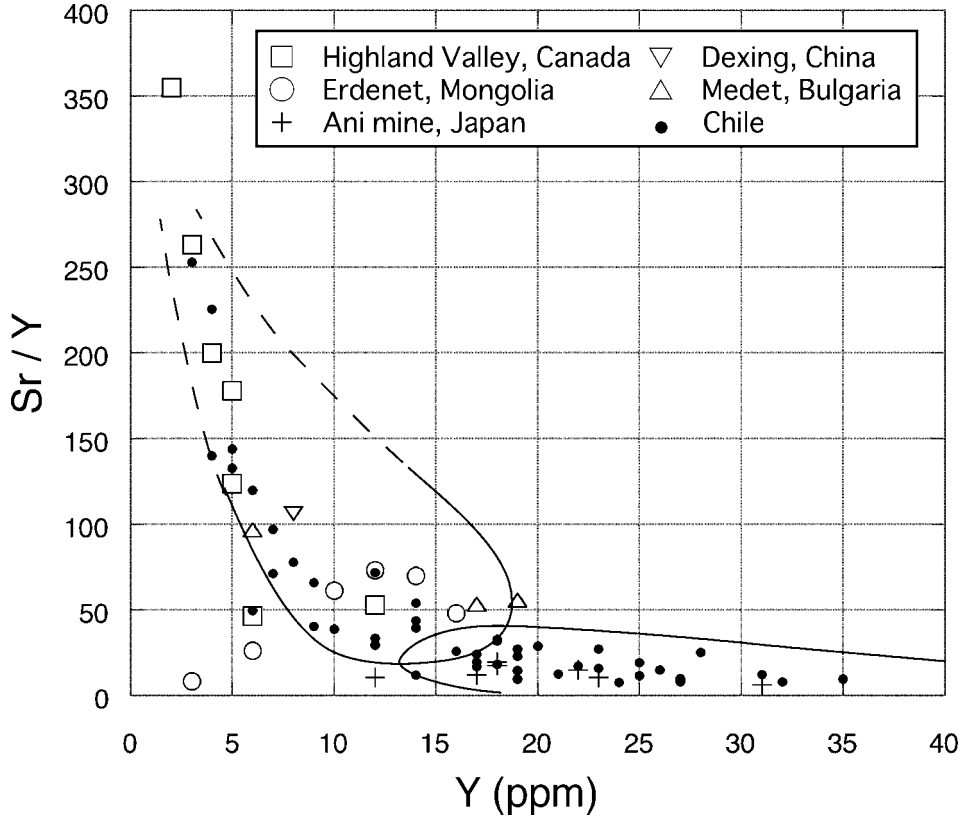


Fig. 14 Sr/Y ratio vs. Y content of the studied granitoids in all the areas. Circled areas are the same as those in Fig. 6.

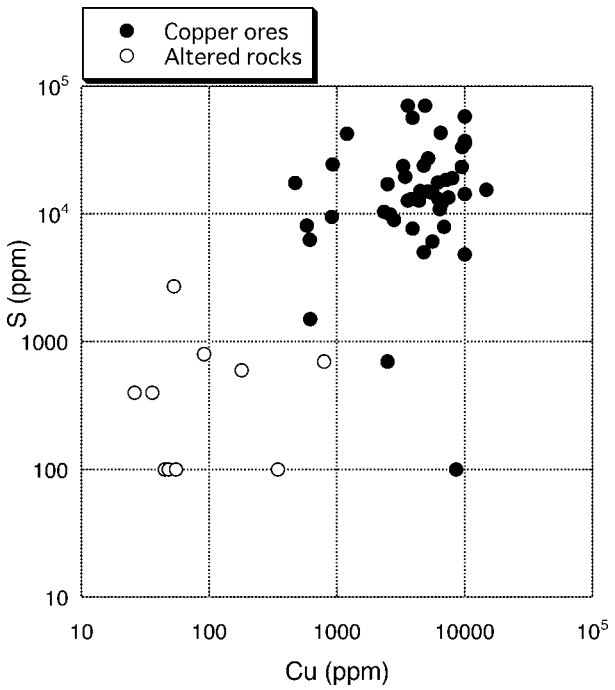


Fig. 15 Copper and sulfur contents of altered and mineralized granitoids at Erdenet open pit. Original data from Naito *et al.* (1996).

of granitoids of orogenic belt. For example, in the Japanese Islands, the ilmenite-series Ryoke batholith in Chubu District has a low average value of 3.6 ppm Cu (n =81, Ishihara and Chappell, 2007).

Magnetite-series granitoids in eastern Shimane Prefecture have an average of 6.9 ppm Cu (n=74), excluding 6 samples of the metasedimentary hornfels (Kanenari and Togiishiyama), and 3 samples of ilmenite-series two-mica granites from the Komaki mine area (Ishihara and Chappell, 2008). The eastern Shimane granitoids are associated with only small base-metal sulfide deposits and a fair amount of molybdenum deposits in the granitoids and surrounding rocks. It is therefore sulfur and metals discharged from the granitoids should be small in amount.

Sulfur content of the studied Chilean granitoids are usually lower than 0.2 % S, except for granodiorite of the underground tunnel at El Salvador mine and porphyry dikes at El Teniente mine (see Appendix 1), because of its volatile character. Sulfur in the magnetite-series magma may possibly be present as sulfate originated ultimately in sea-water sulfate (Sasaki and Ishihara, 1979; Takagi and Tsukimura, 1997) and moved out from the magma chamber to the overlying alteration zones. Such magmatic sulfur is combined with chalcophile element and concentrates chalcopyrite in the alteration zone.

In the studied porphyry copper regions, adakitic and non-adakitic rocks occur together. The non-adakitic granitoids could have been originated from gabbroic lower crust by heating up of adakitic magmas from the upper mantle. Adakitic rocks are most probably generated by partial melting of warm subducted oceanic basalt which was converted to garnet eclogite by subduction. If the basalt was hydrothermally altered originally on the hot and warm sea floor, a primary concentration of copper and sulfur can be easily obtained in the starting materials. Porphyry copper mineralized granitic magmas are possibly generated under such condition and moved upward through low velocity layer of the upper mantle and lower crust where the initial magma mixed with magmas generated there; thus having adakitic and non-adakitic mingled granitoids in the studied porphyry copper regions.

## 8. Concluding Remarks

Plutonic rocks here studied in porphyry copper mineralized areas are characterized by I-type magnetite-series adakitic granitoids, which are most possibly generated by partial melting of down-going oceanic-floor basalt and overlying sediments, which are mixed with non-adakitic granitoids derived from the lower crust gabbroids. These ocean-floor materials, especially when altered along the mid-oceanic ridge, have a great advantage on the ore components of Cu and S.

On the Quaternary volcanic rocks of the Japanese islands, adakitic rocks have not been discovered in the major Quaternary volcanic chain of Northeast Japan, but Daisen, Sanbe-san and others of the Southwest Japan. In the Northeast Japan, the subducting North American Plate is considered as an old and cooled down plate, but in the Southwest Japan, the subducting the Philippine Plate is young and warm, thus having adakitic magmas generated (Ujike *et al.*, 2000). Therefore, magma supply from altered sea-floor basalts and overlying sediments may be a key condition to a large-scale porphyry copper mineralization.

**Acknowledgements:** S. Ishihara is indebted Professor M. Zentilli of Dalhousie University, Y. Watanabe and K. Naito, AIST, for some samples provided, and Dr. B. Munkhtsengel, Mongolian University of Science and Technology, for her guide to the Erdenet mine, Mongolia. Discussion on the adakite geneses with Professor O. Ujike, Toyama University, was helpful to conclude this paper.

## References

Camus, F. (2003) *Geologia de los sistemas porfiricos en los Andes de Chile*. SERNAGEOMIN, 267p.

Casselman, M. J., McMillan, W. J. and Newman, K. M. (1995) Highland Valley porphyry copper deposits near Kamloops, British Columbia: A review and update with emphasis on the Valley deposit. *In Porphyry Deposits of the Northwestern Cordillera of North America*, CIM Spec. Vol., 46, 161-191.

Chappell, B. W. and Hine, R. (2006) The Cornubian batholith: an example of magmatic fractionation on a crustal scale. *Resource Geol*., **56**, 203-244.

Chappell, B. W. and White, A. J. R. (1992) I- and S-type granites in the Lachlan Folded Belt. *Trans. Royal Soc. Edinburgh: Earth Sci.*, **83**, 1-26.

Chappell, B. W., Bryant, C. J., Wyborn, D. White, A. J. R. and Williams, I. S. (1998) High- and low-temperature I-type granites. *Resource Geol.*, **48**, 225-236.

Cobbing, E. J., Pitcher, W. S., Wilson, J. J., Baldock, J. W., Taylor, W. P., McCourt, W. and Snelling, N. J. (1981) The geology of the Western Cordillera of northern Peru. *Inst. Geol. Sci., Overseas Mem.*, **5**, 143p.

Drummond, M. S. and Defant, M. J. (1990) A model of trondhjenite-tonalite-dacite genesis and crustal growth via slab melting: Archean to modern comparisons. *Jour. Geophys. Res.*, **95**, B13, 21503-21521.

Geological Survey of Japan (1984) Research on calc-alkaline magmatism and related mineralization in Chile. *Rept. ITIT Project*, No. 7911, 128p.

Gerel, O. and Munkhtsengel, B. (2005) Erdenetiin Ovoo porphyry copper-molybdenum deposit in northern Mongolia. *In* Seltmann, R., Gerel, O. and Kirwin D., eds., *Geodynamics and Metallogeny of Mongolia with a Special Emphasis on Copper and Gold Deposits*. IAGOD Guidebook Series 11, 85-104.

Gustasfson, L. B. and Quiroga, J. G. (1995) Patterns of mineralization and alteration below the porphyry copper orebody at El Salvador, Chile. *Econ. Geol.*, **90**, 2-16.

Henriquez, F., Nasulund, H. R., Nystrim, J. O., Vivallo, W., Aguirre, R., Dobbs, F. M. and Lledo, H. (2003) New field evidence bearing on the origin of the El Laco magnetite deposit, northern Chile−A discussion. *Econ. Geol.*, **98**, 1497-1500.

Hou, Z., Yang, Z., Qu, X., Meng, X., Li, Z. Beaudoin, G., Rui, Z., Gao,Y. and Zhaw, K. (2009) The Miocene Gandese porphyry copper belt generated during post-collisional extension in the Tibetan Orogen. *Ore Geol. Rev.*, **36**, 25-51.

Imai, A. (2002) Metallogenesis of porphyry Cu deposits of the Western Luzon Arc, Philippines: K-Ar ages, $SO_3$ contents of microphenocrystic apatite and significance of intrusive rocks. *Resource Geol.*, **52**, 147-161.

INGEMMET (2000) *Copper mines in southern Peru: Mina Tintaya (Cuzco), Mina Cerro Verde (Arequipa), Mina Cuajone (Mowuegua) y Mina*

*Toquepala (Tacna)*. Inst. Geol. Minero Metalurgico. Derec. Prospec. Minera, 48p.

Ishihara, S. (1971) Some chemical characteristics of the intrusive rocks of the Bethlehem porphyry copper deposits, B.C., Canada. *Bull. Geol. Surv. Japan*, **22**, 535-546.

Ishihara, S. (2001) Porphyry copper deposits of southern Peru. *Chishitsu News*, no. 563, 6-24 (in Japanese).

Ishihara, S. (2002) Chemical characteristics of the mineralized granitoids (I): Mo and W provinces of the Inner Zone of Southwest Japan. *Bull. Geol. Surv. Japan*, **53**, 657-672 (in Japanese with English abstract).

Ishihara, S. and Chappell, B. W. (2007) Chemical compositions of the late Cretaceous Ryoke granitoids of the Chubu District, central Japan−Revisited. *Bull. Geol. Surv. Japan*, **58**, 323-350.

Ishihara, S. and Chappell, B. W. (2008) Chemical compositions of the Paleogene granitoids of eastern Shimane Prefecture, Sanin District, Southwest Japan. *Bull. Geol. Surv. Japan*, **59**, 225-254.

Ishihara, S. and Tani, K. (2004) Magma mingling/mixing vs. magmatic fractionation: Geneses of the Shirakawa Mo-mineralized granitoids, central Japan. *Resource Geol.*, **54**, 373-382.

Ishihara, S. and Ulriksen, C. E. (1980) The magnetite-series and ilmenite-series granitoids in Chile. *Mining Geol.*, **30**, 183-190.

Ishihara, S., Hashimoto, M. and Machida, M. (2000) Magnetite/ilmenite-series classification and magnetic susceptibility of the Mesozoic-Cenozoic batholiths in Peru. *Resource Geol.*, **50**, 123-129.

Ishihara, S., Ulriksen, C. E., Sato, K. Terashima, S., Sato, T. and Endo, Y. (1984) Plutonic rocks of north-central Chile. *Bull. Geol. Surv. Japan*, **35**, 503-536.

Ishikawa, T. and Nakamura, E. (1994) Origin of the slab component in arc lavas from across-arc variation of B and Pb isotopes. *Nature*, **370**, 205-208.

Japan Mining Association (1968) Ani Mine, *In Ore Deposits of Japan*, 245-251 (in Japanese).

Kamenov, B. K., Uanev, Y., Nedialkov, R., Moritz, R., Peytcheva, I., Von Quadt, A., Stoykov, S. and Zartova, A. (2007) Petrology of Upper Cretaceous island-arc ore-magmatic centers from Central Sregonorie, Bulgaria: Magma evolution and paths. *Geochem. Mineral. Petrol, Sofia*, **45**, 39-77.

Kamiyama, T., Yonebayashi, S., Fukumoto, H., Honma, T. and Aoki, T. (1958) On the geology and ore deposits of the Ani mine, Akita Prefecture, Japan. *Mining Geol.*, **8**, 193-209 (in Japanese with English abstract).

Loiselle. M. C. and Wones, D. R. (1979) Characteristics and origin of anorogenic granites. *Geol. Soc. America, Abstract with Program*, **11**, 468.

Martin, R., Parada, M. A., Palacios, C., Dietrich, A., Schultz, F. and Lehmann, B. (2003) Adakite-like signature of Late Miocene intrusions at the Los Pelambres giant porphyry copper deposit in the Andes of central Chile: metallogenic implications. *Mineral. Deposita*, **38**, 876-885.

McNutt, R. H., Crocket, J. H., Clark, A. H., Caelles, J. C., Farrar, E., Haynes, S. J. and Zentilli, M. (1975) Initial 87Sr/86Sr ratios of plutonic and volcanic rocks of the central Andes between latitudes 26o and 29 o south. *Earth Planet. Sci. Lett.*, **27**, 305-313.

Miller, D. and Groves, D. I (1995) *Potassic igneous rocks and associated gold-copper mineralization*. Lecture Notes in Earth Sciences 56. Springer, 210p.

Moriguti, T. and Nakamura, E. (1998) Across-arc variation of Li isotopes in lavas and implications for crust/mantle recycling at subduction zones. *Earth Planet. Sci. Lett.*, **163**, 167-174.

Mortimer, N. (1986) Two belts of Late Triassic, arc-related, potassic igneous rocks in the North American Cordillera. *Geology*, **14**, 1035-1038.

Muller, D., Heithersay, P. S., and Groves, D. J. (1994) The shoshonite porphyry Cu-Au association in the Goonumbla District, N.S.W., Australia. *Mineral. Petrol.*, **51**, 299-321.

Naito, K., Dejidmaa, D., Dorjigotov, D., Nakajima, T. and Sudo, S. (1996) Geochemical data of granites and ores of Erdenet mine. *In Research on Exploration and Development of Mineral Resources in Mongolia*. ITIT Rept. No. 91-1-3, 103-134.

Nakamura, E., Campbell, I. H. and Sun, S.-S. (1985) The influence of subduction processes on the geochemistry of Japanese alkaline basalts. *Nature*, **316**, 55-58.

Nakayama, K. (2007) Present status of molybdenum mining in the world, with special reference to molybdenum impact to Chilean mining industry. *Chishitsu News*, no. 633, 51-61 (in Japanese).

Ossandon, G. C., Freraut, R. C., Gustafson, L. B., Lindsay, D. D. and Zentilli, M. (2001) Geology of the Chuquicamata mine: A progress report. *Econ. Geol.*, **96**, 249-270.

Oyarzun, J. (2000) Andean metallogenesis: A synoptical review and interpretation. *In* U. G. Cordani *et al.*, eds., *Tectonic Evolution of South America*, 725-753, Rio de Janeiro, Brazil.

Oyarzun, R., Mrques, A., Lillo, J., Lopez, I. and Rivera, S. (2001) Giant versus small porphyry copper deposits of Cenozoic age in northern Chile: adakitic versus normal calc-alkaline magmatism. *Mineral. Deposita*, **36**, 794-798.

Peacock, M. A. (1931) Classification of igneous rock series. *Jour. Geol.*, **39**, 54-67.

Popov, P., Strashimirov, S. and Popov, K. (2003) Geology and metallogeny of the Srednogorie zone

and Panagyurishte ore region. *Soc. Econ. Geol., Guidebook Series*, **36**, 7-26.

Pitcher, W. S., Atherton, M. P., Cobbing, E. J. and Beckensale, R. D. (1985, eds.) *Magmatism at a plate edge: the Peruvian Andes*. Blackie & Son, Ltd. (Glasgow), 328p.

Reich, M., Parada, M. A., Palacios, C., Dietrich A., Schultz, F. and Lehmann, B. (2003) Adakite-like signature of late Miocene intrusions at the Los Pelambres giant porphyry copper deposit in the Andes of central Chile: metallogenic implications. *Mineral. Deposita*, **38**, 376-385.

Sajona, F. G. and Maury, R. C. (1998) Association of adakites with gold and copper mineralization in the Philippines. *C. R. Acad. Sci. Paris, Earth & Planet., Sci.*, **326**, 27-34.

Sasaki, A. and Ishihara, S. (1979) Sulfur isotopic composition of the magnetite-series and ilmenite-series granitoids in Japan. *Contrib. Petrol. Mineral.*, **68**, 107-115.

Shibata, K. and Ishihara, S. (1979) Initial $^{87}Sr/^{86}Sr$ ratios of plutonic rocks from Japan. *Contrib. Mineral. Petrol.*, **79**, 381-390.

Sillitoe, R. H. (1977) Permo-Carboniferous, Upper Cretaceous and Miocene porphyry copper type mineralizations in the Argentine Andes. *Econ. Geol.*, **72**, 99-103.

Sillitoe, R. H. (1992) Gold and copper metallogeny of the central Andes—Past, present and future exploration objectives. *Econ. Geol.*, **87**, 2205-2216.

Sillitoe, R. H. (2003) Iron oxide-copper-gold deposits: an Andean view. *Mineral. Deposita*, **38**, 787-812.

Takagi, T. and Tsukimura, K. (1997) Genesis of oxidized- and reduced-type granites. *Econ. Geol.*, **92**, 81-86.

Tsuchiya, N. and Kanisawa, S. (1994) Early Cretaceous Sr-rich silicic magmatism by slab melting in the Kitakami Mountains, northeast Japan. *Jour. Geophys. Res.*, **99**, B11, 22205-22220.

Tulloch, A. J. and Kimbrough, D. I. (2003) Paired plutonic belts in convergent margins and the development of high Sr/Y magmatism: peninsular Ranges batholith of Baja-California and Median batholith of New Zealand. *Geol. Soc. America, Special Paper*, **374**, 275-295.

Ujike, O., Otoh, S. and Shimizu, M. (2000) Reconstruction of geotectonic structure of eastern Asia before the opening of Japan Sea: 3. an attempt to apply current igneous petrochemical knowledge. *Inst. Northeast Asian Studies Res. Annual. V.* **25**, 181-192 (in Japanese).

Vidal, C. E. (1985) Metallogenesis associated with the Coastal Batholith of Peru: a review. *In* Pitcher, W. S. *et al.*, eds. *Magmatism in a Plate Edge: The Peruvian Andes*. Blackie & Son, Ltd., 243-249.

Watanabe, Y. and Hedenquist, J. W. (2001) Mineralogic and stable isotope zonation at the surface over the El Salvador porphyry copper deposits, Chile. *Econ. Geol.*, **96**, 1775-1797.

Wang, Q., Xu, J-F., Jian, P., Bao, Z-W, Zhao, Z-H., Li, C-F., Xiong X-L., and Ma, J-L. (2006) Petrogenesis of adakitic porphyries in an extensional tectonic setting, Dexing, South China: Implications for the genesis of porphyry copper mineralization. *Jour. Petrol.*, **47**, 119-144.

Yamaoka, K. and Ueda, Y. (1974) K-Ar ages of some ore deposits in Japan. *Mining Geology*, **24**, 291-296 (in Japanese with English abstract).

Zimmerman, A., Stein, H. J., Hannah, J. I., Kozelj, D., Bogdanov, K. and Berza, T. (2008) Tectonic configuration of the Apuyseni-Banat-Timok-Srednogorie belt, Baslkans-South Carpathians, constrained by high precision Re-Os molybdenite ages. *Mineral. Deposita*, **43**, 1-21.

Received April 28, 2010
Accepted September 6, 2010

*Bulletin of the Geological Survey of Japan, vol.61 (11/12), 2010*

# チリ北部，カナダのハイランドバレー，モンゴルのエルデネット，中国の徳興，ブルガリアのメデット，日本の阿仁鉱山における鉱化関連花崗岩類の岩石化学的性質

石原舜三・Bruce W. Chappell

## 要　旨

チリ北部の中生代－新生代花崗岩類を蛍光X線回折法で再分析すると共に，その他地域のポーフィリー型銅鉱床に関係する花崗岩類を同一方法で分析した．チリでは北部，中部，南部の3測線で海岸部（ジュラ紀）から内陸部（第三紀）に至る広域的花崗岩類試料が解析された．ハーカー図において内陸へ増加する傾向を示す成分は$Al_2O_3$，$Na_2O$，$P_2O_5$とSrである．他方，減少の傾向を示す成分はY，全鉄とVである．したがって，高いSr/Y比を持つ花崗岩類が内陸部の若い時代に産出することになる．

世界のその他の対象地域はカナダのB.C.州のハイランドバレー鉱床地域，モンゴルのエルデネット鉱床，中国の徳興鉱床，ブルガリアのメデット鉱床，日本の阿仁鉱床などである．研究した諸岩石は帯磁率測定と$Fe_2O_3$と$FeO$の分析により，全て磁鉄鉱系に属することが明白で，この酸化型マグマの存在は全鉱床で共通する性質である．アルミナ飽和指数（ASI）は1.1より小さく，したがってIタイプに属すると判定された．多くの花崗岩類は$K_2O$-$SiO_2$図上で，高カリウム系列の領域にプロットされるが，ハイランドバレー地域の花崗岩類は低～中Kシリーズに属し，カリウムに乏しい．チリの一部とエルデネット花崗岩類が最もカリウムに富み，ショショナイトも産出する．

その他の成分では，チリの花崗岩類は$P_2O_5$に乏しい．ハイランドバレー鉱床とメデット鉱床の花崗岩類はRbが最低，Srが最大の含有量を持つ．花崗岩類中の微量のCu含有量は大きく変化するが，チリとハイランドバレー鉱床地域の花崗岩類にはその含有量が大きいものが多い．Moは花崗岩類中更に少量であるが，ハイランドバレー，エルデネット，チリの鉱床地域の花崗岩類には，$SiO_2$＝60-65%の中性岩類において5ppm Moを越える高いものがある．

ストロンチウムに富みYに乏しい花崗岩類がチリ，ハイランドバレー，徳興，メデット鉱床地域の鉱化花崗岩類にしばしば認められた．これはアダカイトと認定されるもので，その起源物質はまだ温かい海洋底玄武岩類が，沈みこみ運動によって柘榴石が晶出する高圧化に置かれた後に，部分溶融したものと推定された．海洋底玄武岩が海底熱水変質を受け，微量成分としての銅･硫黄を多く含むものが，ポーフィリー型銅鉱床を形成する可能性が高いものと推定された．日本の阿仁鉱床の花崗岩類はアダカイト質とは無縁であり，この事実は中新世の東北日本で沈み込んだ太平洋プレートは海嶺を遠くはなれ，既に冷却していたためと考えられる．

Appendix 1 Chemical analyses of the Jurassic-Tertiary granitoids in the northern Chile.

| | Jurassic | | | | | | | | Cretaceous |
|---|---|---|---|---|---|---|---|---|---|
| | Varillas Area | | | Tocopilla Area | | | | | Chuqicamata Area |
| Filing No. | 1 | 2 | 3 | 4 | 5 | 6 | 7 | 8 | 9 |
| Sample No. | 79VA03 | 79VA04 | 79VA05 | 79TC11 | 79TC08 | 79TC13 | 79TC10 | 79TC14 | 79CHU07 |
| $SiO_2$ (%) | 58.45 | 65.70 | 66.64 | 48.87 | 54.33 | 53.64 | 57.23 | 63.58 | 59.64 |
| $TiO_2$ | 0.74 | 0.42 | 0.43 | 0.80 | 0.88 | 1.16 | 0.71 | 0.70 | 0.77 |
| $Al_2O_3$ | 16.32 | 16.28 | 15.96 | 17.22 | 17.67 | 16.21 | 16.53 | 15.21 | 16.99 |
| ΣFe2O3 | 7.80 | 4.01 | 3.53 | 11.21 | 9.82 | 10.52 | 7.76 | 6.07 | 6.18 |
| MnO | 0.13 | 0.07 | 0.06 | 0.17 | 0.18 | 0.12 | 0.15 | 0.09 | 0.10 |
| MgO | 3.52 | 1.82 | 1.63 | 7.84 | 4.28 | 4.50 | 4.32 | 2.04 | 3.12 |
| CaO | 6.67 | 3.95 | 3.69 | 11.59 | 8.76 | 8.58 | 7.58 | 4.32 | 5.69 |
| $Na_2O$ | 3.31 | 4.34 | 4.35 | 2.21 | 3.65 | 3.89 | 3.45 | 3.83 | 3.93 |
| $K_2O$ | 2.24 | 2.22 | 2.37 | 0.24 | 0.53 | 1.06 | 1.45 | 2.91 | 2.56 |
| $P_2O_5$ | 0.24 | 0.14 | 0.15 | 0.02 | 0.10 | 0.21 | 0.17 | 0.19 | 0.22 |
| S | 0.03 | <0.01 | <0.01 | <0.01 | <0.01 | <0.01 | <0.01 | <0.01 | <0.01 |
| $H_2O+$ | 1.04 | 1.29 | 0.79 | 0.26 | 0.21 | 1.27 | 1.30 | 1.45 | 0.92 |
| $H_2O-$ | 0.26 | 0.14 | 0.38 | 0.28 | 0.28 | 0.33 | 0.04 | 0.12 | 0.02 |
| $CO_2$ | 0.30 | 0.01 | 0.45 | 0.04 | <0.1 | 0.04 | <0.1 | 0.04 | 0.07 |
| Total | 101.05 | 100.39 | 100.43 | 100.75 | 100.69 | 101.53 | 100.69 | 100.55 | 100.21 |
| Rb (ppm) | 96 | 60 | 50 | 6.1 | 10 | 29 | 45 | 146 | 102 |
| Cs | 5.6 | 2.6 | 4.5 | <1.5 | <1.5 | 1.0 | <1.5 | 4.4 | 6.7 |
| Sr | 360 | 398 | 392 | 356 | 334 | 376 | 269 | 252 | 564 |
| Ba | 271 | 272 | 292 | 73 | 109 | 218 | 259 | 406 | 568 |
| Zr | 165 | 100 | 113 | 13 | 54 | 55 | 48 | 187 | 154 |
| Hf | 6.1 | 4.8 | 3.9 | < 1.9 | 3.0 | 2.2 | < 2.7 | 6.2 | 3.3 |
| Nb | 4.0 | 3.0 | 4.2 | 0.3 | 1.4 | 2.3 | 2.9 | 4.5 | 7.4 |
| Y | 23 | 12 | 10 | 9 | 18 | 22 | 27 | 27 | 18 |
| La | 14 | 15 | 8 | <2 | 2 | 10 | 11 | 14 | 16 |
| Ce | 33 | 29 | 17 | <3 | 11 | 26 | 27 | 38 | 37 |
| V | 177 | 71 | 47 | 391 | 242 | 334 | 147 | 125 | 131 |
| Cr | 64 | 27 | 52 | 155 | 34 | 93 | 222 | 58 | 41 |
| Co | 25 | 13 | 11 | 54 | 32 | 31 | 23 | 15 | 21 |
| Ni | 12 | 12 | 10 | 51 | 5 | 16 | 26 | 10 | 14 |
| Cu | 107 | 75 | 27 | 13 | 109 | 36 | 78 | 247 | 85 |
| Zn | 63 | 46 | 47 | 65 | 68 | 26 | 80 | 40 | 67 |
| Pb | 7 | 9 | 10 | 2 | 3 | 4 | 6 | 8 | 12 |
| Ga | 17.3 | 17.9 | 17.9 | 16.0 | 19.6 | 17.8 | 16.8 | 16.4 | 18.8 |
| Ge | 1.6 | 1.2 | 1.3 | 1.8 | 1.4 | 1.8 | 1.4 | 1.5 | 1.6 |
| As | 2.7 | 2.3 | 0.6 | 1.0 | 0.7 | 5.4 | 3.6 | 10.8 | 3.7 |
| Se | 0.2 | 0.3 | 0.3 | < 0.2 | < 0.1 | < 0.2 | < 0.1 | 0.9 | 0.2 |
| Mo | 1.1 | < 0.2 | 0.4 | 0.3 | 0.7 | 0.7 | 2.1 | 3.0 | 3.5 |
| W | < 1.4 | < 1.1 | 0.9 | < 1.7 | < 1.4 | < 1.3 | 3.6 | 1.6 | < 1.4 |
| Sn | 1.4 | 0.7 | 0.9 | < 0.4 | 0.4 | 0.3 | 0.6 | 1.9 | 1.1 |
| Cd | 0.3 | < 0.2 | < 0.2 | 0.4 | 0.6 | < 0.2 | 0.2 | 0.2 | 0.3 |
| Sb | < 0.5 | < 0.5 | < 0.5 | 0.5 | < 0.5 | < 0.5 | 0.4 | 0.8 | 0.5 |
| Tl | 0.6 | 0.4 | 0.6 | < 0.6 | < 0.6 | < 0.6 | < 0.5 | 0.4 | 0.8 |
| Th | 12.4 | 4.0 | 4.3 | < 0.5 | 0.6 | 5.7 | 4.1 | 15.6 | 12.8 |
| U | 2.7 | 0.7 | 0.6 | 0.6 | 1.8 | 1.4 | 1.4 | 6.2 | 4.4 |
| Mag. Sus. | 25.5 | 12.8 | 19.2 | 73.2 | 41.5 | 28.2 | 22.4 | 31.0 | 36.0 |
| $Fe_2O_3/FeO$ | 0.59 | 0.82 | 0.82 | 0.60 | 0.51 | 0.68 | 0.36 | 0.75 | 0.82 |
| Ga10000/Al | 2.00 | 2.08 | 2.12 | 1.76 | 2.10 | 2.08 | 1.92 | 2.04 | 2.09 |
| ASI | 0.82 | 0.97 | 0.97 | 0.69 | 0.79 | 0.70 | 0.79 | 0.88 | 0.87 |
| Rb/Sr | 0.27 | 0.15 | 0.13 | 0.02 | 0.03 | 0.08 | 0.17 | 0.6 | 0.18 |
| Sr/Y | 15.7 | 33.2 | 39.2 | 39.6 | 18.6 | 17.1 | 10.0 | 9.3 | 31.3 |
| ZrT(°C) | 738 | 731 | 741 | 532 | 641 | 628 | 641 | 769 | 741 |

Note: For high S rocks, equivalent S to form pyrite was subtracted from FeO, which was determined by titration, while the others determined by polarized XRF at GEOMOC, Macquarie University, Sydney, Australia.
Mag. Sus.: Magnetic susceptibility (SI unit) measured by portable device, KT-5.

| | Cretaceous | Tertiary | | Tertiary | | | | |
|---|---|---|---|---|---|---|---|---|
| | Chuqicamata Area | Chuqicamata Area | | Chuqicamata Area | | | Chuqi pit | Arica |
| Filing No. | 10 | 11 | 12 | 13 | 14 | 15 | 16 | 17 |
| Sample No. | 79CHU06 | 79CHU03 | 79CHU05 | 79CHU04 | 79CHU11 | 79CHU12 | CU769 | 80MZH3 |
| $SiO_2$ (%) | 63.05 | 64.34 | 65.07 | 66.05 | 56.72 | 72.28 | 68.63 | 62.82 |
| $TiO_2$ | 0.82 | 0.49 | 0.51 | 0.43 | 1.00 | 0.30 | 0.28 | 0.60 |
| $Al_2O_3$ | 16.02 | 17.25 | 16.38 | 16.23 | 17.91 | 14.00 | 16.26 | 16.95 |
| ΣFe2O3 | 5.52 | 3.91 | 3.88 | 3.58 | 8.14 | 2.46 | 2.93 | 4.90 |
| MnO | 0.09 | 0.06 | 0.05 | 0.04 | 0.14 | 0.06 | 0.03 | 0.06 |
| MgO | 2.10 | 1.48 | 1.54 | 1.28 | 2.48 | 0.80 | 0.71 | 2.52 |
| CaO | 4.12 | 4.42 | 4.06 | 3.66 | 6.78 | 2.30 | 3.00 | 4.96 |
| $Na_2O$ | 3.80 | 4.83 | 4.45 | 4.56 | 4.13 | 3.44 | 4.89 | 3.71 |
| $K_2O$ | 3.82 | 2.39 | 3.04 | 2.90 | 1.47 | 3.83 | 2.89 | 2.61 |
| $P_2O_5$ | 0.21 | 0.21 | 0.19 | 0.17 | 0.31 | 0.08 | 0.13 | 0.18 |
| S | 0.05 | <0.01 | 0.05 | 0.04 | 0.01 | <0.01 | 0.10 | <0.01 |
| $H_2O+$ | 0.77 | 0.60 | 0.74 | 0.83 | 1.44 | 0.52 | 0.48 | 0.82 |
| $H_2O-$ | 0.06 | 0.04 | 0.14 | 0.49 | 0.14 | 0.12 | 0.29 | 0.11 |
| $CO_2$ | <0.1 | 0.07 | 0.04 | 0.07 | 0.04 | 0.07 | 0.09 | 0.06 |
| Total | 100.43 | 100.09 | 100.14 | 100.33 | 100.71 | 100.26 | 100.71 | 100.30 |
| Rb (ppm) | 166 | 69 | 96 | 78 | 48 | 128 | 68 | 95 |
| Cs | 9.5 | 2.2 | 4.1 | 3.2 | 1.4 | 13.5 | 0.9 | 17.6 |
| Sr | 389 | 718 | 608 | 624 | 392 | 168 | 665 | 414 |
| Ba | 658 | 775 | 659 | 763 | 395 | 585 | 828 | 523 |
| Zr | 225 | 110 | 112 | 88 | 139 | 132 | 96 | 150 |
| Hf | 5.7 | 2.5 | 4.2 | 2.5 | 3.7 | 6.7 | 6.1 | 5.3 |
| Nb | 12.7 | 6.4 | 7.9 | 6.5 | 5.9 | 2.3 | 6.2 | 6.2 |
| Y | 26 | 7 | 9 | 8 | 31 | 14 | 5 | 17 |
| La | 26 | 18 | 18 | 17 | 18 | 7 | 12 | 13 |
| Ce | 59 | 35 | 36 | 33 | 46 | 20 | 27 | 30 |
| V | 107 | 61 | 66 | 55 | 146 | 25 | 28 | 104 |
| Cr | 95 | 29 | 33 | 27 | 20 | 39 | 1 | 56 |
| Co | 17 | 13 | 12 | 8 | 20 | 13 | <5 | 17 |
| Ni | 12 | 4 | 8 | 4 | <1 | 2 | < 0.7 | 17 |
| Cu | 20 | 11 | 44 | 113 | 35 | 12 | 445 | 41 |
| Zn | 64 | 43 | 30 | 26 | 67 | 31 | 35 | 46 |
| Pb | 14 | 10 | 9 | 8 | 6 | 14 | 9.0 | 11 |
| Ga | 18.5 | 20.4 | 18.8 | 19.1 | 20.4 | 12.0 | 18.4 | 18.2 |
| Ge | 1.3 | 1.0 | 1.0 | 1.5 | 1.8 | 1.2 | 1.1 | 1.5 |
| As | 10.1 | 1.7 | 1.2 | 2.8 | 1.7 | 1.6 | 3.1 | 2.0 |
| Se | 0.4 | 0.4 | 0.4 | 0.3 | 0.2 | 0.9 | 0.4 | 0.5 |
| Mo | 2.8 | 1.9 | 2.6 | 2.8 | 0.6 | 1.1 | 0.5 | 1.1 |
| W | 2.1 | 0.5 | 2.2 | 1.0 | < 1.4 | 3.1 | 0.7 | 0.9 |
| Sn | 2.0 | 1.9 | 1.3 | 0.8 | 1.3 | 2.8 | 1.0 | 1.2 |
| Cd | < 0.2 | 0.3 | 0.6 | 0.3 | 0.3 | 0.4 | 0.4 | 0.2 |
| Sb | 0.6 | < 0.5 | 0.6 | < 0.5 | < 0.5 | 1.2 | < 0.5 | 0.9 |
| Tl | 0.7 | 0.4 | 1.8 | 0.8 | 0.8 | 3.3 | 1.1 | 1.7 |
| Th | 18.1 | 7.2 | 7.6 | 8.0 | 5.0 | 11.1 | 5.5 | 20.0 |
| U | 5.8 | 3.2 | 3.1 | 3.7 | 1.0 | 2.7 | 0.8 | 4.3 |
| Mag. Sus. | 37.2 | 39.7 | 37.6 | 38.0 | 46.0 | 31.8 | n.d. | 23.8 |
| $Fe_2O_3$/FeO | 1.64 | 1.68 | 1.46 | 1.54 | 0.84 | 0.90 | 3.95 | 0.73 |
| Ga10000/Al | 2.18 | 2.24 | 2.17 | 2.22 | 2.15 | 1.62 | 2.14 | 2.03 |
| ASI | 0.90 | 0.93 | 0.91 | 0.94 | 0.86 | 1.00 | 0.98 | 0.94 |
| Rb/Sr | 0.43 | 0.1 | 0.15 | 0.13 | 0.12 | 0.76 | 0.1 | 0.23 |
| Sr/Y | 15.0 | 103 | 67.6 | 78.0 | 12.7 | 12.0 | 133 | 24.4 |
| ZrT(˚C) | 784 | 729 | 730 | 716 | 727 | 765 | 729 | 755 |

| | Jurassic | | | | | | Cretaceous | | |
|---|---|---|---|---|---|---|---|---|---|
| | Ci Funcho - Caldera Area | | | | | | Copiapo Area | | |
| Filing No. | 18 | 19 | 20 | 21 | 22 | 23 | 24 | 25 | 26 |
| Sample No. | 79SE16 | 79CH01 | 79CH13 | 79CH10 | 79CH12 | 79CH11 | 79CH15 | 79CP07 | 79CP11 |
| $SiO_2$ (%) | 61.83 | 56.06 | 58.70 | 60.97 | 60.92 | 67.62 | 62.53 | 55.28 | 55.07 |
| $TiO_2$ | 0.59 | 1.00 | 0.76 | 0.81 | 0.64 | 0.43 | 0.51 | 0.82 | 0.64 |
| $Al_2O_3$ | 16.52 | 16.71 | 16.99 | 16.20 | 17.33 | 16.20 | 16.43 | 17.80 | 19.15 |
| ΣFe2O3 | 5.20 | 8.71 | 6.98 | 6.83 | 6.42 | 3.39 | 6.08 | 7.92 | 7.47 |
| MnO | 0.06 | 0.11 | 0.11 | 0.10 | 0.12 | 0.07 | 0.11 | 0.12 | 0.19 |
| MgO | 2.47 | 4.49 | 4.04 | 3.00 | 3.27 | 1.62 | 2.49 | 4.42 | 3.68 |
| CaO | 4.94 | 7.77 | 7.43 | 5.98 | 6.42 | 4.01 | 4.71 | 7.86 | 7.80 |
| $Na_2O$ | 3.64 | 3.04 | 3.35 | 3.53 | 3.44 | 4.55 | 4.22 | 3.43 | 3.96 |
| $K_2O$ | 2.57 | 1.29 | 1.34 | 1.49 | 1.47 | 1.58 | 2.20 | 1.41 | 1.07 |
| $P_2O_5$ | 0.16 | 0.15 | 0.12 | 0.12 | 0.10 | 0.14 | 0.10 | 0.12 | 0.20 |
| S | <0.01 | <0.01 | <0.01 | <0.01 | <0.01 | <0.01 | 0.01 | <0.01 | <0.01 |
| $H_2O+$ | 1.83 | 1.33 | 0.38 | 1.32 | 0.42 | 0.36 | 0.70 | 1.28 | 0.82 |
| $H_2O-$ | 0.28 | 0.29 | 0.26 | 0.29 | 0.02 | 0.14 | 0.22 | 0.27 | 0.36 |
| $CO_2$ | 0.39 | 0.17 | 0.18 | 0.12 | 0.04 | 0.04 | 0.26 | 0.15 | 0.04 |
| Total | 100.48 | 101.12 | 100.64 | 100.76 | 100.61 | 100.15 | 100.57 | 100.88 | 100.45 |
| Rb (ppm) | 94 | 53 | 47 | 47 | 46 | 40 | 58 | 31 | 21 |
| Cs | 6.1 | 2.2 | 2.4 | 5.1 | <1.5 | 3.4 | 3.1 | 1.8 | <1.5 |
| Sr | 273 | 289 | 266 | 220 | 257 | 355 | 436 | 850 | 589 |
| Ba | 334 | 223 | 173 | 248 | 258 | 263 | 585 | 326 | 293 |
| Zr | 88 | 92 | 82 | 77 | 130 | 102 | 150 | 65 | 83 |
| Hf | 4.7 | 3.9 | 2.7 | 4.8 | 4.1 | 3.6 | 5.5 | < 3.2 | 2.8 |
| Nb | 3.5 | 4.4 | 3.7 | 4.2 | 5.6 | 4.0 | 5.8 | 4.5 | 3.5 |
| Y | 19 | 25 | 21 | 27 | 32 | 12 | 19 | 12 | 18 |
| La | 12 | 10 | 9 | 8 | 14 | 11 | 15 | 8 | 8 |
| Ce | 25 | 24 | 23 | 20 | 34 | 26 | 36 | 22 | 27 |
| V | 93 | 243 | 178 | 150 | 151 | 41 | 95 | 242 | 136 |
| Cr | 26 | 69 | 97 | 191 | 37 | 42 | 25 | 29 | 19 |
| Co | 12 | 32 | 28 | 18 | 19 | 12 | 15 | 26 | 21 |
| Ni | 4 | 30 | 20 | 13 | 8 | 9 | 1 | 20 | 6 |
| Cu | 149 | 50 | 50 | 44 | 14 | 6 | 10 | 115 | 42 |
| Zn | 83 | 51 | 61 | 66 | 60 | 49 | 55 | 50 | 60 |
| Pb | 17 | 7 | 8 | 6 | 5 | 9 | 7 | 5 | 4 |
| Ga | 16.6 | 17.0 | 18.0 | 16.8 | 17.6 | 17.5 | 17.8 | 19.6 | 20.0 |
| Ge | 1.8 | 1.0 | 1.4 | 1.4 | 1.8 | 1.3 | 1.6 | 1.3 | 1.3 |
| As | 9.6 | 2.7 | 2.4 | 1.1 | 0.8 | < 0.3 | < 0.3 | < 0.3 | < 0.3 |
| Se | 0.6 | 0.1 | 0.2 | < 0.1 | 0.2 | 0.1 | 0.4 | 0.2 | < 0.1 |
| Mo | 0.7 | 1.2 | 1.6 | 0.7 | 0.6 | 0.2 | 1.4 | 0.5 | 0.5 |
| W | 1.7 | 1.5 | < 1.4 | 4.0 | < 1.3 | 1.3 | 0.7 | < 1.4 | < 1.3 |
| Sn | 1.3 | 0.9 | 1.0 | 0.8 | 1.4 | 0.6 | 0.6 | 0.5 | 0.5 |
| Cd | 0.3 | 0.2 | < 0.2 | 0.3 | 0.4 | < 0.2 | < 0.2 | 0.3 | < 0.2 |
| Sb | 0.7 | < 0.5 | 0.3 | < 0.5 | < 0.5 | < 0.5 | < 0.5 | < 0.5 | < 0.5 |
| Tl | 1.3 | 0.9 | 0.8 | 0.7 | 0.4 | 0.9 | 0.5 | 0.6 | 0.4 |
| Th | 4.2 | 4.8 | 5.3 | 4.2 | 2.1 | 3.7 | 7.5 | 3.7 | 1.9 |
| U | 1.6 | 1.3 | 2.2 | 1.4 | 0.6 | < 0.5 | 2.4 | 1.6 | 1.0 |
| Mag. Sus. | 33.6 | 10.7 | 18.2 | 24.6 | 3.7 | 4.6 | 30.0 | 29.9 | 32.4 |
| $Fe_2O_3/FeO$ | 2.00 | 1.67 | 0.29 | 1.99 | 0.37 | 0.70 | 2.24 | 1.93 | 1.01 |
| Ga10000/Al | 1.90 | 1.92 | 2.00 | 1.96 | 1.92 | 2.04 | 2.05 | 2.08 | 1.97 |
| ASI | 0.93 | 0.81 | 0.83 | 0.89 | 0.92 | 0.98 | 0.92 | 0.83 | 0.88 |
| Rb/Sr | 0.34 | 0.18 | 0.18 | 0.21 | 0.18 | 0.11 | 0.13 | 0.04 | 0.04 |
| Sr/Y | 14.4 | 11.6 | 12.7 | 8.2 | 8.0 | 30.0 | 23.0 | 70.8 | 32.7 |
| ZrT(˚C) | 712 | 689 | 685 | 695 | 737 | 735 | 752 | 663 | 685 |

| | Cretaceous | | | | Tertiary | | | | |
|---|---|---|---|---|---|---|---|---|---|
| | Copiapo Area | | | | Copiapo Area | | | El Sarvador Mine | |
| Filing No. | 27 | 28 | 29 | 30 | 31 | 32 | 33 | 34 | 35 |
| Sample No. | 79CP12 | 79CP10 | 79CP09A | 79CP09B | 79CP02 | 79CP05 | 79CP04 | 79PT-L | D110424 |
| $SiO_2$ (%) | 58.34 | 64.83 | 72.92 | 75.28 | 60.90 | 64.36 | 66.54 | 59.02 | 61.66 |
| $TiO_2$ | 0.51 | 0.36 | 0.18 | 0.12 | 0.81 | 0.59 | 0.52 | 1.02 | 0.79 |
| $Al_2O_3$ | 18.43 | 17.19 | 14.41 | 13.24 | 16.53 | 15.90 | 15.52 | 18.02 | 17.63 |
| ΣFe2O3 | 6.67 | 4.32 | 1.97 | 1.27 | 5.89 | 4.61 | 3.99 | 5.79 | 5.10 |
| MnO | 0.16 | 0.12 | 0.04 | 0.03 | 0.11 | 0.08 | 0.07 | 0.02 | 0.03 |
| MgO | 2.79 | 1.43 | 0.58 | 0.31 | 2.76 | 2.26 | 1.68 | 2.22 | 1.58 |
| CaO | 6.87 | 5.01 | 2.33 | 1.40 | 4.70 | 4.12 | 3.63 | 5.21 | 4.52 |
| $Na_2O$ | 3.87 | 4.30 | 3.47 | 2.96 | 4.09 | 3.91 | 3.69 | 4.98 | 5.66 |
| $K_2O$ | 1.18 | 1.73 | 3.74 | 4.89 | 3.65 | 3.42 | 3.81 | 1.57 | 2.30 |
| $P_2O_5$ | 0.19 | 0.17 | 0.06 | 0.04 | 0.22 | 0.16 | 0.13 | 0.34 | 0.26 |
| S | 0.01 | <0.01 | <0.01 | <0.01 | <0.01 | <0.01 | <0.01 | 0.52 | 0.43 |
| $H_2O$+ | 1.17 | 0.49 | 0.29 | 0.27 | 0.52 | 0.71 | 0.51 | 0.45 | 0.53 |
| $H_2O$- | 0.28 | 0.12 | 0.18 | 0.09 | 0.04 | 0.02 | 0.02 | 0.28 | 0.32 |
| $CO_2$ | 0.17 | 0.11 | 0.04 | 0.04 | 0.07 | 0.04 | 0.04 | 0.18 | 0.13 |
| Total | 100.64 | 100.18 | 100.21 | 99.94 | 100.29 | 100.18 | 100.15 | 99.62 | 100.94 |
| Rb (ppm) | 23 | 33 | 79 | 86 | 134 | 141 | 177 | 64 | 55 |
| Cs | 1.7 | 1.5 | 3.7 | 2.9 | 10.3 | 14.3 | 10.5 | 5.4 | 3.5 |
| Sr | 606 | 538 | 274 | 189 | 506 | 417 | 334 | 812 | 719 |
| Ba | 338 | 497 | 577 | 648 | 663 | 620 | 594 | 378 | 472 |
| Zr | 72 | 116 | 72 | 57 | 171 | 149 | 171 | 120 | 105 |
| Hf | 1.7 | 4.1 | 5.1 | 5.1 | 6.6 | 5.6 | 5.5 | 3.8 | 2.7 |
| Nb | 3.4 | 4.3 | 3.4 | 6.2 | 7.0 | 6.7 | 5.8 | 6.7 | 6.9 |
| Y | 14 | 14 | 6 | 19 | 19 | 16 | 17 | 4 | 5 |
| La | 9 | 9 | 7 | 13 | 22 | 18 | 18 | 11 | 12 |
| Ce | 21 | 26 | 11 | 21 | 51 | 39 | 37 | 29 | 33 |
| V | 117 | 63 | 23 | 14 | 121 | 90 | 71 | 94 | 81 |
| Cr | 57 | 33 | 16 | 44 | 43 | 40 | 46 | 39 | 5 |
| Co | 19 | 13 | 8 | 6 | 18 | 19 | 15 | 20 | 12 |
| Ni | 3 | <1 | 2 | 2 | 10 | 12 | 7 | 7 | 3 |
| Cu | 10 | 5 | 75 | 19 | 152 | 88 | 24 | 47 | 36 |
| Zn | 49 | 50 | 18 | 11 | 63 | 68 | 41 | 32 | 27 |
| Pb | 4 | 8 | 9 | 9 | 17 | 22 | 11 | 6 | 3.6 |
| Ga | 19.2 | 16.9 | 13.2 | 11.1 | 18.8 | 19.7 | 16.8 | 26.0 | 23.9 |
| Ge | 1.4 | 1.8 | 1.8 | 1.7 | 1.3 | 1.4 | 1.3 | 1.4 | 1.1 |
| As | 0.6 | < 0.3 | < 0.3 | 0.3 | 3.7 | 15.7 | 7.0 | 0.8 | 1.8 |
| Se | 0.3 | 0.5 | 1.2 | 0.5 | 0.6 | 0.4 | 0.3 | 0.5 | 0.4 |
| Mo | 0.9 | 0.6 | < 0.2 | 0.4 | 13.1 | 4.3 | 1.3 | 1.5 | 122 |
| W | < 1.2 | 0.7 | 3.1 | 3.0 | 2.7 | 4.4 | 2.3 | 1.5 | 10 |
| Sn | 0.8 | 1.1 | 0.9 | 0.9 | 1.7 | 1.4 | 1.5 | 1.2 | 0.7 |
| Cd | 0.3 | 0.7 | 0.5 | 0.2 | 0.3 | < 0.2 | 0.2 | 0.4 | < 0.2 |
| Sb | < 0.5 | 0.8 | < 0.5 | < 0.5 | < 0.5 | 2.2 | 0.9 | < 0.5 | < 0.5 |
| Tl | < 0.5 | 1.6 | 3.0 | 1.9 | 1.7 | 1.8 | 1.1 | 1.2 | 0.4 |
| Th | 2.1 | 3.3 | 8.5 | 10.2 | 14.3 | 16.5 | 20.3 | 2.0 | 0.7 |
| U | 2.0 | 0.9 | 1.9 | 2.4 | 3.8 | 3.8 | 4.3 | < 0.5 | < 0.5 |
| Mag. Sus. | 64.6 | 40.2 | 12.0 | 6.3 | 47.6 | 26.4 | 34.8 | 46.6 | n.d. |
| $Fe_2O_3$/FeO | 0.41 | 1.40 | 1.52 | 1.84 | 1.30 | 1.02 | 1.10 | 1.73 | 3.45 |
| Ga10000/Al | 1.97 | 1.86 | 1.73 | 1.58 | 2.15 | 2.34 | 2.05 | 2.73 | 2.56 |
| ASI | 0.92 | 0.95 | 1.03 | 1.04 | 0.86 | 0.90 | 0.92 | 0.93 | 0.88 |
| Rb/Sr | 0.04 | 0.06 | 0.29 | 0.46 | 0.27 | 0.34 | 0.53 | 0.08 | 0.08 |
| Sr/Y | 43.3 | 38.4 | 45.7 | 10.0 | 26.6 | 26.1 | 19.7 | 203 | 144 |
| ZrT(°C) | 687 | 736 | 719 | 706 | 751 | 752 | 770 | 729 | 714 |

| | Cretaceous | | | | | | | |
|---|---|---|---|---|---|---|---|---|
| | El Sarvador Mine | Valparaiso - Santiago Area | | | | | SE of Santiago Area | |
| Filing No. | 36 | 37 | 38 | 39 | 40 | 41 | 42 | 43 |
| Sample No. | D110432 | 79SA01 | 79SA02 | 79SA09 | 79SA08 | 80SA13 | 79111101 | 81SA12 |
| $SiO_2$ (%) | 61.99 | 51.79 | 57.85 | 54.99 | 66.42 | 61.44 | 71.31 | 60.10 |
| $TiO_2$ | 0.79 | 0.95 | 1.16 | 1.11 | 0.44 | 0.63 | 0.34 | 0.67 |
| $Al_2O_3$ | 17.45 | 17.56 | 17.23 | 15.44 | 15.49 | 16.68 | 14.00 | 17.36 |
| ΣFe2O3 | 4.57 | 10.89 | 6.82 | 9.39 | 3.92 | 5.24 | 2.84 | 5.80 |
| MnO | 0.03 | 0.16 | 0.12 | 0.14 | 0.07 | 0.06 | 0.06 | 0.12 |
| MgO | 1.51 | 4.26 | 3.00 | 3.46 | 1.26 | 2.22 | 0.87 | 2.01 |
| CaO | 4.56 | 9.28 | 5.70 | 7.10 | 3.31 | 4.96 | 2.43 | 4.51 |
| $Na_2O$ | 5.71 | 3.79 | 4.26 | 3.46 | 4.05 | 4.15 | 3.71 | 3.59 |
| $K_2O$ | 1.90 | 0.84 | 3.18 | 3.51 | 3.88 | 2.83 | 3.55 | 4.34 |
| $P_2O_5$ | 0.25 | 0.32 | 0.34 | 0.56 | 0.13 | 0.22 | 0.08 | 0.28 |
| S | 0.46 | <0.01 | <0.01 | <0.01 | <0.01 | 0.19 | <0.01 | 0.01 |
| $H_2O$+ | 0.71 | 0.77 | 0.57 | 1.28 | 1.03 | 0.67 | 0.34 | 1.10 |
| $H_2O$- | 0.45 | 0.06 | 0.10 | 0.08 | 0.08 | 0.26 | 0.16 | 0.18 |
| $CO_2$ | 0.13 | 0.04 | 0.04 | 0.04 | 0.04 | 0.66 | 0.37 | 0.11 |
| Total | 100.51 | 100.71 | 100.37 | 100.56 | 100.12 | 100.21 | 100.06 | 100.18 |
| Rb (ppm) | 66 | 16 | 70 | 95 | 99 | 95 | 128 | 150 |
| Cs | 2.9 | <1.5 | 3.3 | <1.5 | 3.3 | 5.4 | 12.1 | 11.3 |
| Sr | 717 | 639 | 471 | 334 | 290 | 735 | 179 | 699 |
| Ba | 466 | 355 | 607 | 633 | 659 | 734 | 585 | 1810 |
| Zr | 111 | 48 | 355 | 172 | 160 | 146 | 136 | 241 |
| Hf | 2.4 | 3.1 | 9.1 | 4.7 | 5.2 | 4.9 | 6.6 | 6.9 |
| Nb | 7.0 | 2.2 | 15.7 | 6.7 | 2.8 | 7.4 | 3.1 | 14.8 |
| Y | 6 | 23 | 25 | 35 | 17 | 14 | 24 | 28 |
| La | 14 | 10 | 17 | 16 | 8 | 15 | 13 | 34 |
| Ce | 32 | 26 | 44 | 43 | 21 | 35 | 25 | 66 |
| V | 88 | 263 | 134 | 202 | 69 | 98 | 29 | 103 |
| Cr | 3 | 26 | 46 | 42 | 14 | 86 | 17 | 38 |
| Co | 14 | 31 | 22 | 17 | 14 | 20 | 9 | 14 |
| Ni | 4 | 6 | 15 | 7 | <1 | 5 | 3 | <1 |
| Cu | 25 | 27 | 76 | 278 | 18 | 98 | 16 | 62 |
| Zn | 29 | 43 | 72 | 31 | 24 | 44 | 39 | 78 |
| Pb | 3.8 | 5 | 12 | 4 | 6 | 9 | 17 | 30 |
| Ga | 23.9 | 19.0 | 19.4 | 17.2 | 16.4 | 18.6 | 14.4 | 18.1 |
| Ge | 1.0 | 2.0 | 1.4 | 1.9 | 1.5 | 1.2 | 1.5 | 1.5 |
| As | 2.0 | 1.2 | 3.0 | 4.5 | 1.2 | 4.1 | 5.8 | 3.8 |
| Se | 0.2 | 0.3 | 0.3 | < 0.2 | 0.3 | 0.2 | 0.2 | 0.5 |
| Mo | 106 | 0.6 | 2.3 | 3.1 | 0.8 | 1.2 | 1.3 | 1.3 |
| W | 18 | < 1.5 | < 1.5 | 1.0 | 1.5 | 2.6 | 2.6 | 2.5 |
| Sn | 0.8 | 0.8 | 1.4 | 0.7 | 1.5 | 0.8 | 1.9 | 2.8 |
| Cd | < 0.2 | 0.6 | 0.3 | 0.3 | 0.4 | < 0.2 | 0.2 | 0.8 |
| Sb | 0.4 | 0.3 | 0.4 | 0.7 | < 0.5 | 0.5 | 1.8 | 1.0 |
| Tl | 0.5 | 0.6 | 1.0 | 0.4 | 0.7 | 1.2 | 1.1 | 1.4 |
| Th | 1.1 | 3.4 | 9.0 | 8.5 | 9.0 | 10.1 | 14.0 | 20.4 |
| U | < 0.5 | 1.4 | 2.4 | 2.8 | 2.5 | 3.8 | 3.3 | 5.2 |
| Mag. Sus. | n.d. | 130.0 | 35.2 | 28.8 | 15.8 | 34.8 | 16.8 | 10.4 |
| $Fe_2O_3/FeO$ | 5.00 | 1.33 | 0.57 | 0.56 | 0.87 | 1.41 | 0.64 | 1.41 |
| Ga10000/Al | 2.59 | 2.05 | 2.13 | 2.11 | 2.00 | 2.11 | 1.94 | 1.97 |
| ASI | 0.88 | 0.73 | 0.83 | 0.69 | 0.92 | 0.88 | 0.97 | 0.92 |
| Rb/Sr | 0.09 | 0.03 | 0.15 | 0.28 | 0.34 | 0.13 | 0.72 | 0.21 |
| Sr/Y | 120 | 27.8 | 18.8 | 9.5 | 17.1 | 52.5 | 7.5 | 25.0 |
| ZrT(˚C) | 719 | 619 | 800 | 708 | 763 | 742 | 764 | 788 |

| | Tertiary | | | |
|---|---|---|---|---|
| | SE of Santiago Area | Rio Blanco | El Teniente Mine | |
| Filing No. | 44 | 45 | 46 | 47 |
| Sample No. | 81SA11 | 79031402 | ELTN7 | ELTN11 |
| $SiO_2$ (%) | 56.97 | 66.60 | 61.87 | 63.43 |
| $TiO_2$ | 0.99 | 0.51 | 0.49 | 0.50 |
| $Al_2O_3$ | 17.81 | 15.72 | 17.08 | 17.16 |
| ΣFe2O3 | 7.51 | 3.60 | 1.88 | 4.20 |
| MnO | 0.13 | 0.05 | 0.04 | 0.06 |
| MgO | 3.09 | 1.71 | 1.90 | 1.34 |
| CaO | 6.21 | 3.48 | 3.09 | 3.69 |
| $Na_2O$ | 4.50 | 4.48 | 5.73 | 5.79 |
| $K_2O$ | 2.28 | 3.08 | 2.92 | 0.81 |
| $P_2O_5$ | 0.31 | 0.15 | 0.21 | 0.21 |
| S | <0.01 | <0.01 | 1.08 | 0.49 |
| $H_2O$+ | 0.56 | 0.43 | 1.62 | 1.77 |
| $H_2O$- | 0.16 | 0.24 | 0.36 | 0.48 |
| $CO_2$ | 0.15 | 0.07 | 0.73 | 0.97 |
| Total | 100.67 | 100.12 | 99.00 | 100.90 |
| Rb (ppm) | 86 | 87 | 105 | 41 |
| Cs | 4.3 | 3.9 | 3.6 | 13.9 |
| Sr | 577 | 483 | 561 | 760 |
| Ba | 421 | 538 | 516 | 214 |
| Zr | 140 | 115 | 93 | 88 |
| Hf | 4.8 | 3.7 | <7 | <7 |
| Nb | 6.3 | 4.3 | 2.1 | 2.2 |
| Y | 20 | 7 | 4 | 3 |
| La | 15 | 13 | 8 | 13 |
| Ce | 38 | 29 | 20 | 29 |
| V | 131 | 68 | 77 | 78 |
| Cr | 27 | 57 | 23 | 9 |
| Co | 18 | 16 | <5 | <5 |
| Ni | 8 | 11 | 7 | 6 |
| Cu | 94 | 15 | 826 | 793 |
| Zn | 85 | 38 | 32 | 84 |
| Pb | 19 | 10 | 6.0 | 8.7 |
| Ga | 20.3 | 19.1 | 22.7 | 20.8 |
| Ge | 1.6 | 1.3 | 2.1 | 1.1 |
| As | 8.3 | 6.1 | 3.3 | 11.6 |
| Se | 0.5 | 0.4 | 0.4 | 0.3 |
| Mo | 1.7 | 1.7 | 0.9 | 0.7 |
| W | < 1.5 | < 1.0 | 18 | 3.6 |
| Sn | 1.4 | 0.6 | 0.7 | 1.0 |
| Cd | 0.5 | < 0.2 | < 0.2 | < 0.2 |
| Sb | 0.9 | 0.7 | 1.6 | 2.8 |
| Tl | 1.6 | 1.5 | 0.8 | 0.7 |
| Th | 8.8 | 8.5 | 3.2 | 1.9 |
| U | 2.0 | 3.0 | < 0.5 | < 0.5 |
| Mag. Sus. | 45.0 | 27.4 | n.d. | n.d. |
| $Fe_2O_3/FeO$ | 0.66 | 0.93 | infinity | 3.05 |
| Ga10000/Al | 2.15 | 2.30 | 2.51 | 2.29 |
| ASI | 0.84 | 0.92 | 0.94 | 1.00 |
| Rb/Sr | 0.15 | 0.18 | 0.19 | 0.05 |
| Sr/Y | 28.9 | 69.0 | 140 | 253 |
| ZrT(°C) | 723 | 736 | 715 | 721 |

Appendix 2 Chemical analyses of the porphyry Cu-related granitoids in the Highland Valley, southern B.C., Erdenet, Mongolia, Medet, Dexing, China and Bulgaria.

| | Highland Valley, Southern B.C. | | | | | | | Erdenet, Mongolia | | | | |
|---|---|---|---|---|---|---|---|---|---|---|---|---|
| | 68BE01 | 68BE03 | 68BE02 | 68BE04 | TT1411 | TT1401 | TT1501 | 701-1 | 701-2 | ER69 | 701-4 | ER76 |
| SiO2% | 60.96 | 64.13 | 65.78 | 67.40 | 62.77 | 67.21 | 70.89 | 55.34 | 60.51 | 61.48 | 65.80 | 72.16 |
| TiO2 | 0.70 | 0.42 | 0.34 | 0.38 | 0.34 | 0.29 | 0.18 | 1.24 | 1.11 | 0.88 | 0.47 | 0.39 |
| Al2O3 | 16.27 | 16.45 | 16.77 | 16.12 | 16.39 | 16.81 | 15.47 | 17.86 | 14.86 | 16.73 | 16.39 | 16.12 |
| Fe2O3 | 5.32 | 4.29 | 3.18 | 2.55 | 3.01 | 2.94 | 1.83 | 7.78 | 7.07 | 5.41 | 2.96 | 0.23 |
| MnO | 0.06 | 0.03 | 0.03 | 0.02 | 0.05 | 0.06 | 0.03 | 0.11 | 0.10 | 0.08 | 0.04 | <0.01 |
| Mg0 | 2.67 | 1.55 | 1.18 | 1.46 | 1.12 | 1.07 | 0.40 | 3.08 | 3.05 | 2.09 | 1.31 | 0.31 |
| CaO | 5.46 | 4.37 | 4.10 | 2.22 | 4.66 | 3.97 | 2.47 | 6.50 | 4.64 | 4.20 | 2.82 | 0.12 |
| Na2O | 4.82 | 4.22 | 4.79 | 4.86 | 3.73 | 4.70 | 5.10 | 5.57 | 4.08 | 4.92 | 4.19 | 7.06 |
| K2O | 0.97 | 0.55 | 1.45 | 0.81 | 2.79 | 1.80 | 2.22 | 1.10 | 3.01 | 2.74 | 4.75 | 1.62 |
| P2O5 | 0.25 | 0.17 | 0.13 | 0.16 | 0.14 | 0.11 | 0.04 | 0.40 | 0.27 | 0.25 | 0.13 | <0.01 |
| S | <0.01 | 0.33 | 0.04 | 0.81 | 0.03 | <0.01 | 0.02 | 0.04 | 0.04 | <0.01 | 0.02 | 0.02 |
| H2O+ | 2.22 | 2.08 | 1.25 | 2.43 | 1.85 | 0.71 | 0.61 | 0.92 | 1.03 | 0.86 | 0.74 | 1.08 |
| H2O- | 0.34 | 0.44 | 0.25 | 0.00 | 0.10 | 0.11 | 0.25 | 0.11 | 0.16 | 0.21 | 0.12 | 0.27 |
| CO2 | 0.14 | 0.11 | 0.27 | 0.00 | 2.89 | 0.12 | 0.30 | 0.14 | 0.13 | 0.10 | 0.11 | 0.09 |
| Others | 0.17 | 0.40 | 0.26 | 0.72 | 0.22 | 0.22 | 0.23 | 0.23 | 0.33 | 0.39 | 0.26 | 0.09 |
| O=S | | -0.16 | -0.02 | -0.40 | -0.01 | | -0.01 | -0.02 | -0.02 | | -0.01 | -0.01 |
| Total | 100.35 | 99.38 | 99.80 | 99.54 | 100.08 | 100.12 | 100.03 | 100.40 | 100.37 | 100.34 | 100.10 | 99.55 |
| Rb ppm | 23 | 16 | 22 | 24 | 70 | 29 | 32 | 24 | 55 | 47 | 84 | 39 |
| Cs | < 1.5 | 3.0 | 3.0 | < 1.5 | 3.0 | 1.2 | 3.7 | < 1.5 | 5.0 | 2.5 | 5.6 | 1.1 |
| Sr | 635 | 890 | 790 | 800 | 279 | 710 | 620 | 980 | 770 | 880 | 615 | 157 |
| Ba | 174 | 138 | 760 | 230 | 870 | 910 | 850 | 254 | 960 | 860 | 970 | 300 |
| Zr | 106 | 73 | 64 | 77 | 64 | 62 | 61 | 144 | 317 | 260 | 195 | 125 |
| Hf | 3.9 | < 10 | 5.9 | < 15 | < 4.7 | 4.2 | 3.9 | 3.6 | 7.8 | 8.7 | 7.2 | 4.6 |
| Nb | < 0.2 | < 0.2 | < 0.2 | < 0.2 | 0.6 | 0.4 | 1.4 | 4.1 | 4.7 | 0.9 | 1.8 | < 0.2 |
| Y | 12 | 5 | 3 | 4 | 6 | 2 | 5 | 14 | 16 | 12 | 10 | 6 |
| La | 13 | 10 | 4 | 7 | 4 | 2 | 6 | 25 | 19 | 14 | 16 | 5 |
| Ce | 29 | 21 | 12 | 16 | 5 | < 3.0 | 9 | 55 | 45 | 32 | 31 | 11 |
| V | 144 | 96 | 61 | 76 | 67 | 57 | 27 | 173 | 152 | 109 | 62 | 30 |
| Cr | 19 | 4 | 17 | 7 | 5 | 5 | 9 | 3 | 14 | 16 | 26 | 16 |
| Co | 13 | <6 | <5 | <5 | 6 | 12 | 4 | 20 | 18 | 3 | 7 | <2 |
| Ni | 20 | 6 | 5 | 8 | 6 | 6 | 4 | 12 | 15 | 12 | 12 | 3 |
| Cu | 38 | 1830 | 318 | 4410 | 422 | 3.9 | 220 | 51 | 180 | 740 | 61 | 7.4 |
| Zn | 45 | 60 | 28 | 36 | 33 | 39 | 26 | 60 | 66 | 171 | 30 | 12 |
| Pb | 5.2 | 7.9 | 6.5 | 5.4 | 4.7 | 9.4 | 9.5 | 14 | 14 | 13 | 12 | 13 |
| Ga | 15.6 | 16.9 | 15.6 | 15.0 | 16.3 | 16.0 | 15.0 | 20.6 | 17.1 | 19.2 | 15.5 | 18.2 |
| Ge | 1.2 | 1.6 | 1.3 | 1.3 | 0.8 | 1.0 | 1.6 | 0.9 | 1.0 | 1.1 | 0.9 | 1.4 |
| As | 3.3 | 1.8 | < 0.3 | < 0.3 | < 0.3 | < 0.3 | < 0.3 | < 0.4 | 0.6 | < 0.4 | < 0.4 | < 0.3 |
| Se | 0.5 | 0.8 | 0.7 | 1.1 | 1.1 | 2.0 | 1.0 | 0.9 | 0.7 | 0.6 | 0.8 | 0.5 |
| Mo | 14.0 | 5.4 | 4.5 | 15.1 | 5.8 | 4.5 | 3.6 | 7.1 | 18.3 | 9.7 | 10.1 | 2.4 |
| W | <1 | <2 | <1 | <2 | <1 | 0.9 | <1 | <2 | <2 | <2 | 0.9 | 7.3 |
| Sn | 1.3 | 1.6 | 1.3 | 1.8 | 1.0 | 2.4 | 1.5 | 2.1 | 1.8 | 1.5 | 1.6 | 1.8 |
| Cd | 0.6 | 0.4 | 0.5 | 2.0 | 0.4 | 0.9 | 0.2 | < 0.2 | < 0.2 | 0.3 | < 0.2 | < 0.2 |
| Sb | 0.8 | 1.0 | 1.0 | 0.6 | 1.1 | 1.3 | < 0.5 | < 0.5 | 0.5 | < 0.5 | < 0.5 | 0.8 |
| Tl | 2.5 | 3.2 | 3.0 | 3.3 | 3.6 | 5.7 | 3.3 | 3.3 | 2.8 | 2.4 | 2.7 | 1.7 |
| Bi | 1.2 | 1.3 | 1.2 | 0.8 | 2.1 | 3.5 | 1.5 | 1.1 | 0.7 | 0.8 | 0.9 | 1.7 |
| Th | 5.9 | 2.7 | 2.6 | 2.4 | 2.5 | 2.8 | 2.1 | 3.8 | 6.5 | 5.7 | 8.4 | 1.0 |
| U | 6.0 | 6.2 | 5.6 | 5.1 | 5.2 | 5.1 | 5.6 | 7.3 | 7.4 | 3.6 | 5.6 | 0.8 |
| Mag. Sus. | 46.4 | 37.8 | 29.2 | 0.3 | 13.1 | 35.2 | 21.2 | 30.0 | 33.6 | 23.0 | n.d. | 0.1 |
| Fe2O3/FeO | 0.90 | 0.53 | 0.77 | n.d. | 0.90 | 0.92 | 1.00 | n.d. | n.d. | n.d. | n.d. | n.d. |
| Ga*10000/Al | 1.8 | 1.9 | 1.8 | 1.8 | 1.9 | 1.8 | 1.8 | 2.2 | 2.2 | 2.2 | 1.8 | 2.1 |
| ASI | 0.86 | 1.06 | 0.99 | 1.25 | 0.93 | 0.99 | 1.01 | 0.81 | 0.81 | 0.89 | 0.96 | 1.19 |
| Rb/Sr | 0.04 | 0.02 | 0.03 | 0.03 | 0.25 | 0.04 | 0.05 | 0.02 | 0.07 | 0.05 | 0.14 | 0.25 |
| Sr/Y | 52.9 | 178.0 | 263.3 | 200.0 | 46.5 | 355.0 | 124.0 | 70.0 | 48.1 | 73.3 | 61.5 | 26.2 |
| Zr°C | 714 | 716 | 698 | 739 | 689 | 697 | 702 | 715 | 798 | 793 | 783 | 776 |

| | | Dexing | Medet, Bulgaria | | |
|---|---|---|---|---|---|
| | ER03 | TX1901 | MD02 | MD03 | MD04 |
| SiO2% | 72.66 | 62.94 | 56.84 | 62.24 | 69.18 |
| TiO2 | 0.37 | 0.48 | 0.65 | 0.53 | 0.26 |
| Al2O3 | 15.72 | 15.01 | 17.85 | 15.97 | 14.90 |
| Fe2O3 | 1.86 | 4.52 | 5.44 | 5.08 | 2.70 |
| MnO | <0.01 | 0.05 | 0.07 | 0.09 | 0.08 |
| Mg0 | 0.34 | 2.70 | 2.94 | 2.10 | 0.91 |
| CaO | <0.01 | 4.60 | 5.47 | 4.25 | 3.27 |
| Na2O | 0.36 | 3.90 | 3.65 | 3.65 | 3.52 |
| K2O | 4.55 | 3.34 | 3.43 | 2.36 | 4.32 |
| P2O5 | 0.07 | 0.25 | 0.40 | 0.28 | 0.13 |
| S | 1.38 | 0.10 | 0.43 | 0.47 | <0.01 |
| H2O+ | 1.32 | 0.89 | 1.84 | 1.79 | 0.32 |
| H2O- | 0.00 | 0.02 | 0.27 | 0.38 | 0.15 |
| CO2 | 0.00 | 0.71 | 0.13 | 0.17 | 0.11 |
| Others | 1.01 | 0.30 | 0.40 | 0.25 | 0.18 |
| O=S | -0.69 | -0.05 | -0.21 | -0.23 | |
| Total | 98.95 | 99.76 | 99.60 | 99.38 | 100.03 |
| Rb ppm | 83 | 90 | 115 | 54 | 165 |
| Cs | 3.9 | 6.0 | < 1.5 | < 1.5 | 5.1 |
| Sr | 25 | 850 | 1060 | 910 | 580 |
| Ba | 660 | 1140 | 450 | 440 | 441 |
| Zr | 104 | 109 | 85 | 117 | 65 |
| Hf | < 16 | 1.6 | < 7.8 | 4.2 | 3.3 |
| Nb | 3.2 | 6.4 | 4.0 | 5.2 | 1.6 |
| Y | 3 | 8 | 19 | 17 | 6 |
| La | 12 | 23 | 25 | 23 | 22 |
| Ce | 17 | 42 | 57 | 50 | 28 |
| V | 91 | 76 | 277 | 153 | 61 |
| Cr | 13 | 87 | <1 | <1 | 1 |
| Co | <4 | 11 | <8 | 10 | 10 |
| Ni | 4 | 26 | 4 | 2 | 4 |
| Cu | 5690 | 5.7 | 980 | 134 | 8.6 |
| Zn | 95 | 24 | 46 | 32 | 23 |
| Pb | 4.9 | 9.4 | 6.0 | 8.7 | 12 |
| Ga | 13.3 | 16.1 | 18.1 | 16.3 | 14.6 |
| Ge | 1.3 | 1.2 | 1.8 | 2.0 | 1.8 |
| As | 62 | 0.3 | < 0.3 | < 0.4 | < 0.4 |
| Se | 3.0 | 0.8 | 2.8 | 1.8 | 0.8 |
| Mo | 1220 | 3.5 | 4.1 | 3.1 | 3.0 |
| W | 13.5 | <1 | <2 | <2 | <1 |
| Sn | 6.2 | 1.6 | 1.6 | 1.8 | 1.6 |
| Cd | < 0.2 | < 0.2 | < 0.2 | < 0.2 | < 0.2 |
| Sb | 2.2 | 0.9 | < 0.5 | < 0.5 | < 0.5 |
| Tl | 2.5 | 3.1 | 3.3 | 3.2 | 3.3 |
| Bi | 3.2 | 1.4 | 1.6 | 1.1 | 1.2 |
| Th | 6.5 | 18.2 | 9.8 | 11.5 | 16.7 |
| U | < 0.5 | 11.1 | 8.1 | 8.7 | 12.0 |
| Mag. Sus. | 0.2 | 21.6 | 27.6 | 40.4 | 31.2 |
| Fe2O3/FeO | n.d. | 1.19 | 0.89 | 1.12 | 1.50 |
| Ga*10000/Al | 1.6 | 2.0 | 1.9 | 1.9 | 1.9 |
| ASI | n.d. | 0.82 | 0.91 | 0.98 | 0.91 |
| Rb/Sr | 3.32 | 0.11 | 0.11 | 0.06 | 0.28 |
| Sr/Y | 8.3 | 106.3 | 55.8 | 53.5 | 96.7 |
| Zr°C | 818 | 714 | 698 | 743 | 695 |

Appendix 3　Chemical analyses of the Cu-related granitoids in the Ani mine, Japan.

| | 71AN20 | 71AN07 | 71AN02 | 71AN03 | 71AN08 | 71AN12 | 71AN19 | 71AN18 |
|---|---|---|---|---|---|---|---|---|
| SiO2 | 55.89 | 64.81 | 65.72 | 67.21 | 64.97 | 67.14 | 60.66 | 51.24 |
| TiO2 | 0.86 | 0.55 | 0.55 | 0.50 | 0.78 | 0.51 | 0.89 | 0.87 |
| Al2O3 | 16.94 | 16.30 | 16.05 | 15.54 | 15.22 | 15.34 | 15.92 | 16.41 |
| ΣFe2O3 | 8.51 | 4.33 | 3.95 | 3.65 | 5.16 | 3.91 | 7.41 | 12.58 |
| Fe2O3 | 3.35 | 2.32 | 2.07 | 1.80 | 5.16 | 3.91 | 7.41 | 12.58 |
| FeO | 4.49 | 2.52 | 1.65 | 1.85 | n.d. | n.d. | n.d. | n.d. |
| MnO | 0.23 | 0.09 | 0.08 | 0.07 | 0.21 | 0.09 | 0.19 | 0.38 |
| MgO | 4.37 | 1.99 | 1.41 | 1.28 | 2.22 | 1.59 | 3.19 | 5.05 |
| CaO | 6.32 | 1.06 | 3.18 | 2.61 | 1.96 | 1.34 | 0.79 | 0.69 |
| Na2O | 3.02 | 4.28 | 3.80 | 3.85 | 4.35 | 4.24 | 1.71 | 1.13 |
| K2O | 1.97 | 4.52 | 3.46 | 3.77 | 3.07 | 4.23 | 4.62 | 6.89 |
| P2O5 | 0.25 | 0.19 | 0.19 | 0.16 | 0.19 | 0.18 | 0.17 | 0.19 |
| S | 0.09 | 0.04 | <0.01 | <0.01 | 0.03 | <0.01 | 0.50 | <0.01 |
| H2O+ | 1.71 | 1.86 | 1.60 | 1.09 | 1.80 | 1.43 | 3.76 | 4.92 |
| H2O- | 0.26 | 0.23 | 0.24 | 0.13 | 0.08 | 0.00 | 0.22 | 0.35 |
| CO2 | 0.15 | 0.04 | 0.11 | 0.22 | 0.16 | 0.09 | 0.67 | 0.26 |
| O=S | -0.04 | -0.02 | | | -0.01 | | -0.25 | |
| Sum | 100.53 | 100.27 | 100.34 | 100.08 | 100.19 | 100.09 | 100.45 | 100.96 |
| Rb | 59 | 111 | 96 | 109 | 80 | 130 | 127 | 152 |
| Cs | 3.7 | 5.6 | 4.0 | 3.6 | 3.9 | 3.4 | 10.7 | 1.4 |
| Sr | 334 | 243 | 359 | 321 | 196 | 207 | 124 | 32 |
| Ba | 523 | 1340 | 834 | 927 | 778 | 1015 | 1225 | 1370 |
| Zr | 67 | 272 | 260 | 234 | 209 | 226 | 110 | 76 |
| Hf | 2.4 | 7.5 | 7.2 | 6.3 | 7.8 | 6.0 | 4.3 | 4.0 |
| Nb | 3.9 | 8.7 | 8.7 | 8.7 | 8.9 | 8.3 | 4.7 | 2.6 |
| Y | 22 | 23 | 18 | 18 | 31 | 17 | 12 | 22 |
| La | 8 | 15 | 18 | 18 | 14 | 16 | 4 | <2 |
| Ce | 24 | 39 | 38 | 41 | 38 | 39 | 12 | 8 |
| V | 211 | 70 | 63 | 52 | 92 | 41 | 223 | 258 |
| Cr | 89 | 37 | 307 | 25 | 19 | 110 | 108 | 65 |
| Co | 21 | 11 | 11 | 8 | 9 | 14 | 10 | 24 |
| Ni | 21 | 4 | 6 | 4 | 5 | 5 | 16 | 16 |
| Cu | 86 | 91 | 4 | 96 | 74 | 2 | 324 | 222 |
| Zn | 124 | 75 | 57 | 62 | 125 | 72 | 136 | 215 |
| Pb | 26 | 8 | 11 | 25 | 18 | 12 | 7 | 12 |
| Ga | 17.0 | 16.2 | 17.5 | 16.8 | 15.3 | 14.4 | 17.0 | 16.1 |
| Ge | 1.4 | 0.9 | 1.3 | 1.3 | 1.2 | 0.6 | 1.0 | 0.9 |
| As | 0.5 | < 0.3 | < 0.4 | < 0.5 | 0.9 | < 0.4 | 1.3 | < 0.5 |
| Se | < 0.2 | 0.3 | < 0.1 | 0.2 | < 0.1 | < 0.1 | < 0.1 | < 0.2 |
| Mo | 1.7 | 1.6 | 1.4 | 1.4 | 1.6 | 0.3 | 26 | 0.2 |
| W | 3.0 | 2.3 | 4.4 | 0.7 | < 1.5 | 4.0 | 5.0 | < 2.3 |
| Sn | 0.8 | 1.7 | 0.6 | 7.5 | 1.5 | 1.2 | 1.5 | 3.6 |
| Cd | 0.9 | 0.5 | < 0.2 | < 0.2 | 0.6 | 0.8 | 0.8 | 0.4 |
| Sb | 0.6 | 0.5 | < 0.5 | 0.4 | 1.0 | 1.4 | 0.6 | < 0.5 |
| Tl | 0.6 | 1.2 | 1.0 | 0.7 | 0.8 | 1.5 | 1.2 | 1.1 |
| Bi | < 0.4 | < 0.3 | 0.6 | < 0.3 | < 0.3 | 0.5 | < 0.3 | < 0.5 |
| Th | 3.1 | 8.7 | 10.3 | 10.9 | 5.3 | 10.4 | 3.9 | 1.2 |
| U | 0.4 | 2.4 | 2.8 | 2.1 | 1.6 | 2.2 | 0.5 | < 0.5 |
| Mag. Sus. | 46.2 | 26.8 | 33.8 | 30.0 | 23.2 | 5.2 | >10.3 | 10.3 |
| Fe2O3/FeO | 0.8 | 0.9 | 1.1 | 1.0 | n.d. | n.d. | n.d. | n.d. |
| Ga*10000/A | 1.9 | 1.9 | 2.1 | 2.0 | 1.9 | 1.8 | 2.0 | 1.9 |
| ASI | 0.91 | 1.18 | 1.02 | 1.03 | 1.08 | 1.10 | 1.72 | 1.55 |
| Rb/Sr | 0.2 | 0.5 | 0.3 | 0.3 | 0.4 | 0.6 | 1.0 | 4.7 |
| Sr/Y | 15.2 | 10.6 | 19.9 | 17.8 | 6.3 | 12.2 | 10.3 | 1.5 |
| Zr°C | 683 | 841 | 818 | 812 | 809 | 818 | 793 | 749 |